Results in Engineering 27 (2025) 106613

Contents lists available at ScienceDirect

Results in Engineering

journal homepage: www.sciencedirect.com/journal/results-in-engineering

Research paper

OS-RFODG: Open-source ROS2 framework for outdoor UAV dataset generation

Imen Jarraya [a,*], Mohamed Abdelkader [a], Khaled Gabr [a], Muhammad Bilal Kadri [a], Fatimah Alahmed [a], Wadii Boulila [a], Anis Koubaa [b]

[a] Robotics and Internet of Things Laboratory, College of Computer and Information Sciences, Prince Sultan University, Riyadh, 12435, Saudi Arabia
[b] Alfaisal University, Riyadh, Saudi Arabia

ARTICLE INFO

Keywords:
UAV localization
Dataset generation
ROS2 framework
Geospatial mapping
Sensor data synchronization

ABSTRACT

Accurate localization is critical for Unmanned Aerial Vehicles (UAVs) in applications such as military operations, search and rescue, and environmental monitoring. However, existing open-source UAV datasets often lack the synchronization and detail necessary for high-precision localization in complex outdoor environments. To address this, the Open Source ROS2 Framework for Outdoor UAV Dataset Generation (OS-RFODG) is proposed as a cost-effective tool for generating multi-sensor UAV localization datasets. These datasets support the benchmarking of various localization methods, including learning-based models and sensor fusion techniques. OS-RFODG integrates Robot Operating System 2 (ROS2) with the PX4 autopilot, Gazebo simulator, and QGroundControl (QGC) to collect synchronized data from Light Detection and Ranging (LiDAR), Global Positioning System (GPS), Inertial Measurement Unit (IMU), camera, and barometer sensors. Geospatial data from Quantum GIS (QGIS) and Blender is used to create detailed 3D digital maps, improving terrain realism and spatial accuracy. Validation was conducted in the Makkah region of Saudi Arabia, featuring six UAV flights across diverse terrains, with distances ranging from 3.23 km to 14.70 km. In the first evaluation, GPS tracks were exported as Keyhole Markup Language (KML) files and overlaid onto Google Earth imagery, showing strong alignment with real-world terrain. In the second evaluation, the framework achieved RMSE values between 13.59 m and 19.50 m in trajectory alignment relative to a digital 3D GeoTIFF map. Additionally, image-based localization using SIFT keypoint matching reached precision scores up to 0.8964 and spatial RMSEs below 1.34 m. OS-RFODG open-source architecture ensures reproducibility and easy integration into UAV research workflows.

1. Introduction

The rapid advancement of autonomous aerial systems, particularly Unmanned Aerial Vehicles (UAVs), has significantly expanded their applications across various domains, including environmental monitoring, disaster response, and surveillance [1–4]. A fundamental requirement for the effective deployment of these systems is precise localization within a global or local reference frame. This process, commonly referred to as localization or geolocation, enables UAVs to navigate complex environments, execute predefined missions, and interact safely with their surroundings. Global Navigation Satellite Systems (GNSS), such as the U.S. Global Positioning System (GPS), Russia's GLONASS, Europe's Galileo, and China's BeiDou, are widely utilized in UAV applications to provide accurate, real-time geolocation and navigation capabilities. However, in GNSS-denied environments such as urban canyons, dense forests, or indoor areas, reliable position estimation is hindered by signal degradation, uneven terrain, and the limitations of individual sensors [5]. To address GNSS-denied scenarios, UAVs rely on the real-time fusion of complementary sensors. IMUs provide high-rate motion data but are prone to drift. Vision-based methods, such as SLAM and visual odometry, extract features for mapping but degrade in low-texture or poorly lit environments. LiDAR offers precise three-dimensional profiling but is affected by rain or fog [6,7]. Radar provides coarse yet consistent range sensing under all weather conditions. Additional sensors such as ultra-wideband radios, time-of-flight modules, barometers, magnetometers, and optical or thermal cameras contribute data that enhances localization [8,9].

Reliable UAV localization in GNSS-denied environments hinges on real-time fusion of heterogeneous sensor data, as no single modality offers sufficient accuracy in isolation [10].

* Corresponding author.
E-mail address: ijarraya@psu.edu.sa (I. Jarraya).

https://doi.org/10.1016/j.rineng.2025.106613
Received 20 January 2025; Received in revised form 22 July 2025; Accepted 4 August 2025

Available online 8 August 2025
2590-1230/© 2025 The Authors. Published by Elsevier B.V. This is an open access article under the CC BY-NC-ND license (http://creativecommons.org/licenses/by-nc-nd/4.0/).

Experts in robotics, aerospace, and geospatial systems increasingly rely on multi-sensor fusion to achieve centimeter-level precision.

GNSS-based positioning, although widely adopted in UAV navigation, faces significant limitations in environments such as urban canyons, dense forests, and mountainous regions. In such conditions, GNSS signals are highly susceptible to multipath effects, signal obstructions, and atmospheric interference, often leading to localization errors exceeding several meters. These inaccuracies compromise mission safety and reliability, particularly in applications requiring high-precision maneuvering. To overcome these limitations, multi-sensor fusion techniques are indispensable.

Datasets like INSANE have demonstrated the enhanced robustness achieved through such fusion, especially across diverse environments, including Mars-analog sites and indoor–outdoor transitions. Specifically, INSANE showed that reliable UAV localization and mapping can be attained even in magnetically distorted and GNSS-deprived Mars-analog environments by synchronizing data from GNSS, LiDAR, IMU, cameras, and barometers [11]. The dataset's evaluation further confirmed sub-meter accuracy in GNSS-denied segments using visual-inertial odometry fused with LiDAR, and highlighted the importance of redundant sensing to maintain continuity during sensor dropouts.

Moreover, elevation-aware datasets incorporating Digital Elevation Models (DEM), Digital Surface Models (DSM), and Digital Terrain Models (DTM) are critical for correcting vertical drift and terrain-induced localization errors [12]. This is particularly important in fields like precision agriculture, where GNSS disruptions can result in misalignment, yield loss, or ecological harm. The OS-RFODG framework directly addresses these challenges by generating synchronized, geo-referenced, multi-sensor datasets, offering a reproducible and scalable foundation for evaluating UAV localization methods in GNSS-denied environments

Building on this foundation, advancing resilient localization algorithms in GNSS-denied environments necessitates access to realistic and elevation-aware datasets. This need becomes increasingly critical as UAVs are expected to perform autonomous tasks with minimal external guidance and under unpredictable conditions. The effectiveness of classical filters like the Extended Kalman Filter (EKF), Unscented Kalman Filter (UKF), and Particle Filter (PF), along with optimization-based techniques such as factor-graph smoothing and Graph SLAM, and learning-based models including LSTM networks and attention-driven architectures, is closely tied to the availability of realistic and elevation-aware datasets [13–16]. Moreover, the design and benchmarking of these models must account for variations in terrain, sensor characteristics, and mission constraints. Robust development and evaluation of these methods require datasets that accurately reflect real-world complexity. This includes the integration of synchronized sensor data and geospatial elevation information such as DEM, DSM, and DTM. Ground-truth trajectories should be precisely aligned with actual terrain and captured across diverse lighting, topographic, and weather conditions. To meet these challenges, researchers require datasets that not only ensure sensor synchronization but also emulate the operational variability encountered during real UAV deployments. Combining visual and non-visual modalities with elevation-aware mapping is essential for designing, validating, and benchmarking reliable UAV localization algorithms in GNSS-denied scenarios.

Despite notable advances in UAV localization research, existing open-source datasets continue to exhibit several critical limitations that hinder the development and benchmarking of multi-sensor fusion algorithms. A common shortcoming is the lack of precise temporal alignment across heterogeneous sensor streams, which results in cumulative drift and reduced accuracy during dynamic flight maneuvers [5]. Furthermore, many datasets fail to capture realistic environmental disturbances such as lighting variations, wind gusts, precipitation, and airborne particulates. This omission restricts the generalization capability of models trained exclusively under ideal conditions [17]. Elevation modeling also remains inadequate in most publicly available datasets. Few resources provide comprehensive terrain representations such as DEMs, DSMs, and DTMs, which are essential for correcting vertical drift and exploiting topographic cues during navigation [6].

While synthetic datasets typically include accurate ground truth, they often lack authentic sensor noise, hardware variability, and real-world dynamics. On the other hand, field-collected datasets better reflect operational complexity but are usually limited in geographic extent and environmental diversity [11]. Additional limitations include insufficient diversity in sensor types and hardware platforms, the absence of metadata concerning calibration and sensor installation geometry, and a lack of support for extended flight durations or mission-specific conditions. Moreover, the absence of standardized benchmarks and unified evaluation protocols for terrain-aware multi-sensor fusion continues to hinder reproducibility and fair performance comparisons [10,8]. To overcome these challenges, future datasets must provide full temporal synchronization, support a wide range of sensors and environmental scenarios, incorporate detailed terrain layers, and adopt standardized formats and metrics that facilitate rigorous and reproducible evaluation.

Motivated by the limitations of current UAV datasets, we introduce OS-RFODG, an open-source framework based on ROS 2 for the systematic generation of UAV datasets. OS-RFODG offers an integrated pipeline that combines terrain modeling, flight simulation, and synchronized multi-sensor data collection. GeoTIFF elevation maps are processed using QGIS and converted into textured 3D meshes in Blender. UAV missions are defined in QGroundControl, executed through PX4, and simulated over realistic terrain in Gazebo. ROS 2 middleware ensures precise microsecond-level synchronization across sensors, including IMU, RGB camera, LiDAR, barometer, and GPS. The resulting datasets include temporally aligned sensor measurements, elevation queries, ground-truth trajectories, and image sequences, saved in both ROS 2 bag and CSV formats to support reproducible research and performance evaluation. The main contributions of this work are as follows:

- Unified dataset generation: OS-RFODG provides a modular ROS 2-compatible platform for creating datasets that are spatially and temporally synchronized, integrating visual and non-visual sensors.
- Terrain-aware simulation: The framework supports realistic mission design and simulation using high-resolution GeoTIFF elevation data to capture natural topographic variability.
- Reproducibility and extensibility: OS-RFODG enables repeatable experiments and allows researchers to customize sensor configurations and mission scenarios according to their needs.

It is important to note that while this paper demonstrates OS-RFODG using the Makkah region of Saudi Arabia, the framework is designed to support global applicability. Researchers can utilize the framework to generate datasets for any geographical region by importing appropriate GeoTIFF elevation data and satellite imagery. This flexibility enables the creation of training datasets that reflect the specific geographical and environmental characteristics relevant to each research application or deployment scenario.

The remainder of this paper is organized as follows. Section 2 reviews related work on UAV localization in GNSS-denied settings. Section 3 outlines the architecture and methodology of OS-RFODG. Section 4 presents the experimental validation, including dataset generation over the Makkah region, flight path comparisons, RMSE-based elevation accuracy analysis, and visual trajectory inspection. Section 5 concludes with a summary and potential research extensions.

2. Related works

Research on UAV dataset generation for global localization can be grouped into three acquisition modalities: free and commercial data platforms (Table 1), simulation environments, crowd-sourced and field-collected repositories, and large-scale multi-sensor benchmarks.

Table 1
Overview of tools and platforms for generating UAV localization datasets.

Tool/Platform	Description	Type
RTKLIB	Open-source software for Real-Time Kinematic (RTK) GPS processing, enhancing GPS data accuracy	Free/Open Source
OpenDroneMap	Open-source software for processing aerial imagery to generate maps and 3D models	Free/Open Source
Google Earth Engine	Cloud-based platform offering satellite imagery and Digital Elevation Models for large-scale geospatial analysis	Free/Open Source
QGIS	Free GIS software for analyzing and visualizing geospatial data	Free/Open Source
Blender	Open-source 3D modeling and visualization software, used for creating digital terrain models	Free/Open Source
u-blox	High-precision GPS modules for enhanced UAV localization accuracy	Paid
Pix4D	Photogrammetry software for creating 3D maps and models from aerial images	Paid
Velodyne LiDAR	LiDAR sensors offering precise 3D mapping and distance measurements for obstacle detection	Paid
DroneDeploy	UAV flight planning and data processing platform, including advanced mapping and analysis tools	Paid
Emlid Reach RTK	RTK GPS modules for high-accuracy positioning in real-time	Paid

These sources differ in the range of sensors supported in their spatial and temporal resolution, in their geographic coverage, and in their cost of access [18], [19], [20], [21], [22].

2.1. Free and commercial platforms

Several free and open-source platforms provide the foundational tools and datasets needed for UAV localization research. Researchers can access community-curated image collections, sensor logs, and geospatial processing utilities without licensing fees. For example, Kaggle hosts the UAV-VisLoc visual localization dataset with frame-level annotations for obstacle avoidance and computer vision training [23]. GitHub repositories such as CTU-MRS offer synchronized ROS bag recordings of visual-inertial and LiDAR data from cooperative multi-vehicle flights, complete with sub-millisecond timestamp alignment via Chrony, camera–IMU calibration files, and example tmuxinator sessions for RViz playback [24]. Tools like OpenDroneMap convert aerial imagery into orthomosaics, point clouds, 3D models, and DEMs directly from the command line [25], while RTKLIB processes raw GNSS data for real-time kinematic corrections [26]. Google Earth Engine provides API access to global satellite imagery and DEM archives, USGS EarthExplorer enables bulk download of aerial photographs and elevation products [27], [28] [29]. QGIS handles GeoTIFF reprojection and terrain mesh exports, and Blender transforms GIS meshes into textured 3D scenes for simulation [30], [31]. These resources lower the barrier to entry but often require additional integration work to achieve full multi-sensor synchronization and standardized data formats.

Commercial platforms deliver turnkey UAV mapping, photogrammetry, and real-time localization solutions at a financial cost. DroneDeploy offers cloud-based workflows for photogrammetry, 3D modeling, and site inspection, featuring integrated GIS overlays [32], [33]. Pix4D offers desktop and cloud photogrammetry software (Pix4Dmapper, Pix4Dmatic) with RTK-enabled modules for survey-grade DEM, DSM, and point-cloud creation [34]. u-blox produces RTK GNSS modules optimized for UAV navigation and centimeter-level accuracy [35], [36]. Velodyne LiDAR manufactures lightweight sensors (Puck LITE) for real-time 3D mapping and obstacle detection on drones [37]. Emlid Reach receivers support multi-band RTK and PPK workflows with tilt compensation and centimeter accuracy [38]. These commercial solutions guarantee higher precision and vendor support but introduce financial barriers and potential vendor lock-in due to proprietary hardware, software dependencies, and licensing fees.

2.2. Simulation environments

Simulation environments are indispensable tools for developing and testing UAV systems without the need for physical hardware. They enable researchers to model complex scenarios, test algorithms, and generate synthetic datasets under controlled conditions. Recent advances have enhanced the realism and capabilities of these simulators, particularly in the context of outdoor UAV localization.

Gazebo is a widely used open-source robotics simulator that offers a rich set of features for UAV simulation. It supports integration with ROS 2 and provides realistic physics and sensor models. A recent study presents a ROS 2-based simulator framework for tethered UAV-UGV marsupial systems in Gazebo, demonstrating its applicability for UAV research [39]. Building upon the capabilities offered by Gazebo, AirSim, developed by Microsoft, is a high-fidelity simulator for drones and autonomous vehicles. Built on Unreal Engine, it provides realistic environments and supports both software-in-the-loop (SITL) and hardware-in-the-loop (HITL) simulations. AirSim has been utilized for various applications, including reinforcement learning and computer vision research [40]. Moreover, X-Plane is a flight simulator known for its accurate flight dynamics and realistic environments. It has been extended to include functionalities such as complex wind dynamics, ground effect, and accurate real-time weather, making it suitable for UAV pilot training and control algorithm testing [41].

These simulation platforms allow for fine-grained control over environmental conditions, sensor configurations, and UAV dynamics. They are invaluable for generating synthetic datasets, testing algorithms, and accelerating the development of UAV systems. However, it is essential to recognize that simulations may not accurately capture all real-world complexities, such as sensor noise and environmental variability. Therefore, it is recommended to complement simulation studies with real-world experiments to ensure robust localization performance of UAVs.

2.3. Recent UAV dataset studies

Recent progress in UAV geo-localization, especially under GNSS-denied conditions, has led to the emergence of a wide range of datasets employing diverse sensor modalities. These datasets are typically categorized based on whether they incorporate mapping resources such as DEMs or DSMs, and the nature of the sensors used, including visual, non-visual, or a combination of both. Table 2 summarizes the most recent and representative datasets.

Several modern datasets focus exclusively on visual or non-visual sensing modalities without incorporating explicit terrain references. For

Table 2
UAV localization datasets.

Name & Reference	Source	Sensors	UAV Viewpoint	Pose DoF	Open Source	Elevation Data
Wyard et al. 2022 [46]	UAV RGB+Multispectral	RTK-GPS, IMU, RGB, Multispectral	Top View	6-DoF	No	Yes
Wu et al. 2024 [47]	3D Textured Model, DSM	RGB, Depth, IMU, DSM	Arbitrary	6-DoF	Yes	Yes
Yao et al. 2024 [48]	Digital Twin Imagery	RGB (Drone/Satellite)	Cross-view	2-DoF	Yes	Yes
Shi et al. 2019 [45]	GRAL	RGB, LiDAR, Depth, IMU	Arbitrary	6-DoF	Yes	Yes
Barone et al. 2022	GRAL, CVUSA	RGB, LiDAR, IMUs	Arbitrary	6-DoF	Yes	Yes
Xu et al. 2024 [17]	UAV-VisLoc	RGB, Satellite	Arbitrary	6-DoF	Yes	No
Xiao et al. 2023 [42]	Thermal Imagery + Satellite	Thermal, IMU	Arbitrary	6-DoF	Yes	No
Patel et al. 2020 [49]	Google Earth Sim	RTK-GPS, IMU	Arbitrary	4-DoF	No	No
Chen et al. 2021 [50]	Google Earth Sim	GPS, IMU	Arbitrary	6-DoF	No	No
Gurgu et al. 2022 [51]	Simulated Imagery	RTK-GPS	Top View	2-DoF	Yes	No
Yan et al. 2022 [52]	Rendered/Real Images	RTK-GPS, GCPs	Arbitrary	6-DoF	Yes	No
Cisneros et al. 2022 [53]	Real Imagery	RTK-GPS, GCPs	Arbitrary	6-DoF	Yes	No
Zhai et al. 2017 [54]	CVUSA	RGB (Ground/Satellite)	Cross-view	2-DoF	Yes	No
Zheng et al. 2020 [55]	Univ-1652	RGB Cameras	Top View	2-DoF	Yes	No
Wang et al. 2025 [44]	Custom Aerial Imagery	RGB	Arbitrary	6-DoF	No	No
Brommer et al. 2022 [43]	INSANE	RGB, IMUs, RTK-GPS	Arbitrary	6-DoF	Yes	No
Ours (2025)	OS-RFODG	GeoTIFF (DTM, DSM and DEM), RGB, LiDAR, IMU, GPS, Barometer	Arbitrary	6-DoF	Yes	Yes

instance, Xu et al. (2024) [17] present a large-scale dataset, UAV-VisLoc, that utilizes both free-source and field-collected data to improve UAV visual localization in GNSS-denied environments. This dataset addresses the limitations of existing datasets that often focus on small geographic areas or are confined to urban regions with distinct textures. UAV-VisLoc comprises 6,742 drone images and 11 satellite maps, covering various terrains across 11 locations in China. The images, captured by multi-rotor and fixed-wing UAVs at altitudes from 400 to 2,000 meters, include metadata such as latitude, longitude, altitude, and capture dates. The dataset features diverse topographies, including villages, towns, cities, rivers, farms, and hills, providing a broad range of scenarios for training and testing UAV localization models. In addition, images were captured at various heading angles and seasons (summer and fall), which enhanced the data diversity for real-world applications. Satellite maps are sourced from Google Earth with a spatial resolution of 0.3 meters, ensuring high-quality reference data for precise localization tasks. UAV-VisLoc is particularly valuable for developing localization algorithms that perform robustly across different regions and altitudes. While it offers varied flight conditions and terrains, the dataset primarily focuses on China, limiting the generalizability of models trained solely on this data. Furthermore, it does not include sensor fusion data, such as IMU or LiDAR, which could enhance UAV localization, especially in complex environments where additional sensor data is crucial for accurate positioning.

In a related effort, Xiao et al. (2023) [42] introduce a dataset comprising thermal imagery captured using FLIR Boson cameras during nighttime UAV flights over 33 km^2. To address the lack of paired thermal and satellite data, they developed a Thermal Generative Module (TGM) that produces 79,950 synthetic and over 49,000 real image pairs. Their geo-localization framework combines domain adaptation, contrast enhancement, Superpoint+Superglue descriptors, and gravity-guided PnP RANSAC, achieving 92% Recall@1 and sub-15 meter L2 error. However, elevation data is not explicitly provided, and uniform terrains pose challenges for precise localization.

Similarly, the INSANE dataset, developed by Brommer et al. (2022) [43], provides an extensive suite of synchronized sensor data designed for UAV research in various operational scenarios, including indoor, outdoor, and Mars analog environments. This dataset spans over 600 GB and comprises 26 flight sequences covering a total of 2.5 kilometers. The UAV platform is equipped with 18 distinct sensors, including high-resolution stereo and monocular navigation cameras, dual RTK-GNSS modules, and three spatially distributed IMUs, enabling the capture of detailed motion and environment data. Ground truth trajectory data is obtained with centimeter-level positional and sub-degree angular precision, relying on motion capture systems in indoor settings and dual RTK solutions outdoors. In addition to flight data, the dataset includes raw calibration files, static sensor recordings, and vibration profiles, supporting a wide range of research applications such as sensor fusion, real-time localization, and SLAM. Despite its rich sensor configuration and precise annotations, the dataset does not incorporate standardized elevation data such as GeoTIFF-based DEMs or DSMs, which may restrict its applicability for terrain-informed localization and terrain-relative navigation studies.

In a complementary effort, Wang et al. (2025) [44] contributed a custom dataset optimized for the Lightv8nPnP model. It supports high-speed UAV localization with real-time inference at 186 frames per second and sub-6 cm 3D accuracy. The dataset does not include elevation data but is suitable for embedded UAV systems operating in structured environments. Furthermore, Shi et al. (2019) [45] and Barone et al. (2022) expanded the GRAL dataset, integrating multiple modalities such as RGB, LiDAR, depth, and IMU. While open-source, the datasets lack consistently formatted DEM or elevation data, constraining their utility for terrain-aware methods.

Transitioning to datasets that explicitly incorporate elevation data, Wyard et al. (2022) [46] developed an object-based image analysis (OBIA) pipeline for landfill land-cover classification using RGB and multispectral UAV imagery. A Digital Surface Model (DSM) was generated via UAV photogrammetry to provide elevation data. The processing workflow integrated GRASS GIS and R within a Python environment, enabling the incorporation of textural and contextual features alongside spectral information. The classification scheme distinguished 11 land-cover classes, including various types of waste, vegetation, and bare soil. Using a Random Forest classifier, the study achieved an overall classification accuracy of 88.5%, with the addition of contextual features yielding a 6% improvement over spectral-only models. While comprehensive and methodologically robust, the dataset is site-specific and not publicly accessible, limiting its utility for broader geolocation or terrain-aware benchmarking studies.

Expanding the scope to publicly available resources, Wu et al. (2024) [47] introduced UAVD4L, a comprehensive dataset designed to facilitate six degrees of freedom (6-DoF) UAV localization in GPS-denied environments.

The dataset addresses key limitations of prior efforts, such as restricted geographic coverage, limited viewpoint diversity, and insufficient ground-truth accuracy. UAVD4L spans approximately 2.5 million square meters of diverse urban and rural landscapes and includes a high-resolution textured 3D reference model reconstructed from aerial oblique imagery. This model supports the generation of synthetic RGB and depth images, along with a Digital Surface Model (DSM) for terrain representation. Real-world query images were acquired from five distinct UAV flight trajectories, covering altitudes from 50 m to 200 m and pitch angles between 15° and 70°, enabling a wide range of acquisition conditions. For ground-truth annotation, the dataset employs a semi-automated approach combining Structure-from-Motion (SfM) techniques with manual tie-point correction, ensuring accurate 6-DoF pose labels. The localization pipeline integrates offline synthetic data with online visual localization, using SuperPoint and SuperGlue for feature matching and a gravity-guided PnP RANSAC for pose estimation. This framework achieved 93.88% image retrieval accuracy and 96.68% localization success within a 5-meter and 5-degree margin, establishing UAVD4L as a robust benchmark for visual localization in GNSS-denied settings.

In addition, Yao et al. (2024) [48] introduced VDUAV, a cross-view geo-localization dataset built using digital-twin technology. It aligns UAV-captured images with satellite imagery over urban and rural scenes, facilitating 2-DoF localization. Although elevation is not directly provided, terrain variation is indirectly captured. Their VRLM model achieved 83.35% mean average precision at top-20 image retrieval.

In summary, although recent UAV datasets have advanced visual and sensor-based localization, they often lack synchronized multi-sensor data and standardized terrain models required for reliable terrain-aware navigation. To overcome these limitations, we present the OS-RFODG framework, which enables the generation of high-quality, open-source datasets suited to complex outdoor environments. It integrates RGB imagery, LiDAR (Light Detection and Ranging), IMU (Inertial Measurement Unit), GPS (Global Positioning System), and barometric data, all precisely synchronized and aligned with GeoTIFF-based DEM, DTM, and DSM layers created using QGIS and Blender. OS-RFODG distinguishes itself by supporting consistent, terrain-informed data generation and robust benchmarking of hybrid localization algorithms in GNSS-denied scenarios.

3. Open-source OS-RFODG framework and methodology

This study introduces the OS-RFODG framework, a modular and open-source, tool-driven methodology designed to generate high-fidelity UAV datasets in geospatially accurate environments. The pipeline is structured into two core phases, as illustrated in Fig. 1. The first phase focuses on terrain preprocessing, including the extraction of satellite imagery and elevation models, and the generation of textured 3D meshes representing real-world landscapes using QGIS and Blender. The second phase involves simulation-based UAV mission execution within Gazebo, where PX4 handles autopilot dynamics and QGroundControl specifies elevation-aware waypoints. ROS 2 is used for real-time communication and sensor synchronization across GPS, IMU, LiDAR, barometer, and RGB camera streams. Each phase leverages open-source tools in a coordinated workflow to ensure spatial accuracy, visual realism, and precise temporal alignment. The generated datasets comprise georeferenced RGB imagery and precisely time-aligned multi-sensor telemetry, exported in standardized CSV and PNG formats. By facilitating the replication of realistic terrain conditions and mission-specific flight profiles, the framework ensures experimental reproducibility and supports rigorous benchmarking across a wide range of UAV localization and navigation research scenarios.

3.1. Preliminary step: area identification and georeferenced map preparation

The initial phase of the OS-RFODG framework involves defining a specific geographic area for simulation, guided by the intended application or research objectives. This area is delineated using region boundaries, specified by the latitude and longitude coordinates of the upper-left (northwest) and lower-right (southeast) corners. These coordinates establish the spatial extent for data extraction and ensure consistency across all subsequent data layers and processing steps. The defined region boundaries serve as a reference for extracting both elevation and visual data from publicly available repositories. By applying this uniform spatial extent, all retrieved datasets, whether elevation-based or image-based, are clipped and georeferenced to the same coordinate framework, enabling seamless integration. This process yields three essential files that form the digital foundation of the simulation environment:

- A GeoTIFF file (`.tif`) containing digital elevation or surface model data with embedded coordinate referencing.
- A PNG file (`.png`) providing high-resolution satellite imagery aligned to the same spatial footprint.
- A Collada file (`.dae`) containing the 3D textured terrain model suitable for import into the simulation engine.

These assets collectively define the virtual terrain with geospatial accuracy and high visual fidelity. They are critical inputs for downstream processes in the OS-RFODG pipeline, including terrain modeling, sensor integration, and realistic UAV dataset generation.

3.1.1. Georeferenced map preparation with QGIS

In this context, QGIS is instrumental in acquiring, processing, and preparing the geospatial data necessary for realistic UAV simulations [56], [57]. The process begins with gathering high-quality geospatial data, specifically DEMs and DSMs, from reliable public databases or governmental sources, such as the United States Geological Survey (USGS), the National Aeronautics and Space Administration (NASA) and the European Space Agency (ESA). These trusted sources provide accurate and relevant data specific to the research region.

The acquired DEMs and DSMs are typically provided in the GeoTIFF (`.tif`) format, a widely recognized georeferenced raster image format ideal for storing spatial data. GeoTIFF files embed essential geospatial metadata, such as elevation values and coordinate information, which are crucial for maintaining spatial accuracy within simulations. The compatibility of GeoTIFF with QGIS facilitates efficient processing and organization of detailed graphics, streamlining its integration into UAV simulation environments. This ensures that the geospatial data utilized is both precise and well-suited for accurate terrain representation in UAV applications. Several factors influence the resolution and quality of the GeoTIFF files:

- **Quality of the Source Data**: The initial resolution and accuracy of the data, such as whether it comes from high-resolution satellite imagery or lower-quality aerial photographs. Higher-quality source data results in better detail in the final GeoTIFF.
- **Sensor Specifications**: The capabilities of the sensors that captured the data play a significant role. For example:
  - **Spatial Resolution**: The size of the smallest distinguishable features. A sensor that captures images at 1 m resolution yields more detail than one capturing at 10 m.
  - **Spectral Resolution**: The ability of the sensor to capture data at different wavelengths, affecting the richness of the information collected about surface materials.
- **Scale of the Data**: The scale at which the data is represented in QGIS impacts the level of detail in the GeoTIFF. Data processed at a

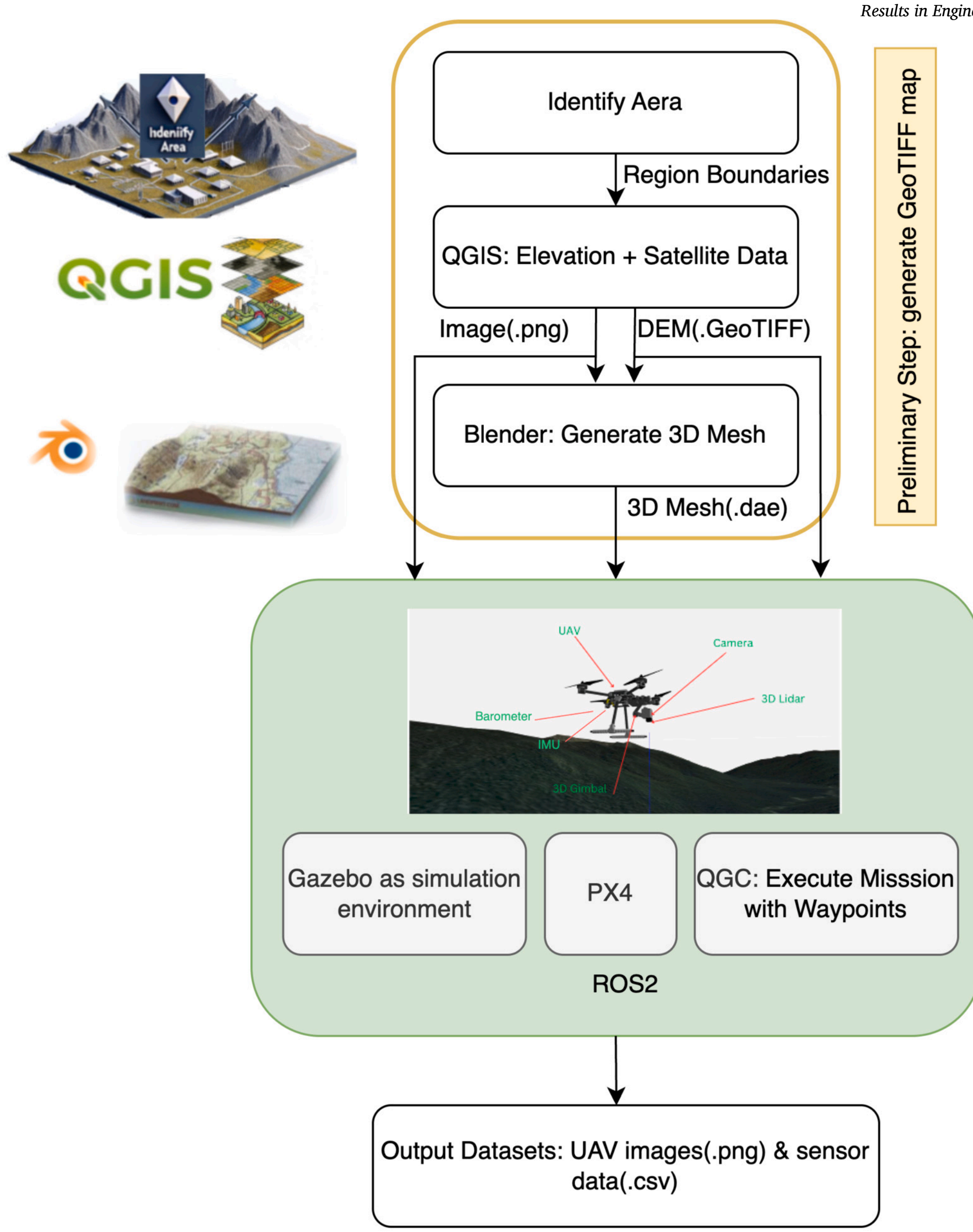

Fig. 1. Overview of the OS-RFODG framework pipeline. The upper block (yellow) illustrates the geospatial terrain preprocessing phase using QGIS and Blender. The lower block (green) represents the ROS 2-based simulation environment, which integrates PX4, Gazebo, and QGroundControl for multi-sensor data generation. The output comprises temporally aligned UAV imagery and sensor telemetry.

larger scale (e.g., 1:5.000) provides more detail than data processed at a smaller scale (e.g., 1:50.000).

- **Interpolation Methods**: The technique used to estimate pixel values during processing can significantly impact the resulting image quality. Common interpolation methods in QGIS include:
  - **Nearest Neighbor**: Fast and maintains original pixel values but may produce a blocky appearance.
  - **Bilinear Interpolation**: Averages the values of the nearest four pixels, resulting in smoother images.
  - **Cubic Convolution**: Uses a weighted average of the nearest 16 pixels for even smoother results, though it may introduce artifacts.
- **Coordinate Reference System (CRS)**: The choice of CRS can affect how data is projected and displayed. An appropriate CRS ensures that spatial relationships between features are accurately maintained.
- **Data Processing Parameters**: Settings applied during data processing, such as pixel size specified for the GeoTIFF export, also influence the final resolution.

Once the geospatial data is processed and validated, it is exported as a GeoTIFF file. This georeferenced file serves as a detailed digital model of the region and forms the foundation for the next stage in Blender, where it will be transformed into a 3D terrain model.

3.1.2. 3D terrain modeling in blender

The processed elevation and satellite data from QGIS [58,59], stored in the GeoTIFF (`.tif`) format, are imported into Blender, a powerful open-source tool for 3D modeling. This import allows Blender to effectively transform the geospatial data into a high-fidelity 3D terrain model. Upon importing the GeoTIFF file, Blender interprets the elevation values, generating a detailed 3D mesh that accurately represents the area's topography, including features such as hills, valleys, and other natural landforms. This mesh provides a realistic depiction of the landscape, eliminating the need for complex manual adjustments, as Blender's displacement modifier facilitates a seamless conversion of elevation data into three-dimensional structures. In parallel, the visual accuracy of the terrain model is significantly enhanced through texture mapping using satellite imagery sourced from QGIS.

In summary, Blender's UV mapping tools align satellite imagery with 3D mesh contours, creating realistic surface textures (e.g., vegetation, rocks) that enhance visual fidelity for high-quality simulations. Once the 3D terrain model is finalized, it is exported from Blender in the `.dae` (Collada) format, which is widely compatible with simulation platforms like Gazebo. This format preserves both the model's geometric and texture data, ensuring smooth integration into UAV simulation workflows. The exported model maintains structural accuracy along with essential visual details, creating a robust environment for testing UAV navigation and localization techniques. Integrating DEM and satellite imagery from QGIS into Blender creates a georeferenced 3D model that ensures spatial accuracy and realism for UAV dataset generation and algorithm testing.

3.2. Open-source ROS2 framework for outdoor UAV dataset generation

The OS-RFODG framework incorporates a 3D mesh derived from GeoTIFF data, which accurately captures essential real-world terrain features. This mesh is imported into Gazebo, an open-source robotics simulation platform integrated with ROS 2 Humble [60], [61], creating a foundational environment for UAV simulation. Within Gazebo, the virtual landscape is further enhanced with realistic elements, such as varied elevations, obstacles, and intricate terrain features, effectively mirroring actual field conditions to support comprehensive UAV testing and data generation.

3.2.1. Simulation environment and flight control integration

This open-source ROS2 framework for UAV dataset generation integrates key components: Gazebo, providing a realistic simulation environment; PX4, the flight control firmware managing UAV operations; and QGC, the ground control station for mission planning and management. These components are connected via MAVROS, a MAVLink-ROS interface that bridges ROS and MAVLink communication protocol, enabling seamless data synchronization and control. MAVROS facilitates bidirectional communication, allowing ROS to send commands to the UAV through MAVLink and receive real-time telemetry data. This interface supports essential operations such as waypoint management, sensor data collection, and flight status monitoring, ensuring that all system components remain in synchronization and respond accurately to simulated conditions.

The process begins with mission planning in QGC, the ground control station that allows operators to define mission parameters, including waypoints, target altitudes, and flight paths. QGC then sends these high-level mission commands to PX4 over the MAVLink protocol [62], setting the UAV's mission objectives. This setup supports both automated and manual control, allowing operators flexibility in testing UAV behaviors across various scenarios. During the mission, QGC continuously receives telemetry feedback from PX4, enabling real-time monitoring, adjustments to mission parameters, or manual intervention if required.

Once QGC transmits the mission commands, PX4, the core flight control firmware, receives these commands and translates them into precise control actions for the UAV. Running in Software-in-the-Loop (SITL) mode, PX4 interfaces with both QGC and Gazebo, acting as the intermediary that interprets mission instructions and adjusts the UAV's behavior accordingly. PX4 relies on real-time environmental feedback from Gazebo to adapt its control actions dynamically, ensuring that the UAV can respond to terrain changes, navigate obstacles, and maintain altitude based on simulated environmental cues.

PX4 manages its communication with other simulation components through several interfaces:

- MAVLink Interface: Connects to API/offboard control for autonomous UAV navigation based on external commands, which is essential for developer testing and allows for real-time adjustments via external applications or scripts.
- QGC Connection: Receives mission instructions, including waypoints and flight paths, which PX4 then executes within the Gazebo environment, facilitating remote mission management.
- Telemetry Exchange with Gazebo: Ensures that UAV responses accurately reflect the simulated environment, allowing PX4 to synchronize with Gazebo for real-time environmental feedback.

With mission commands in place and PX4 controlling the UAV, Gazebo serves as the environment provider where the UAV performs its mission in a controlled yet realistic setting. The MAVLink protocol enables real-time data exchange between Gazebo and PX4, with UDP communication supporting telemetry and control data synchronization. Gazebo continuously supplies PX4 with simulated environmental feedback, allowing the UAV to respond to interactions such as altitude adjustments, terrain following, and obstacle navigation [63]. This seamless interaction is essential for rigorous testing and evaluation of UAV navigation and localization algorithms, as it ensures that the UAV's responses are aligned with the complexity of the simulated terrain.

Within the OS-RFODG framework, QGC, PX4, and Gazebo form a synchronized control and feedback loop, supporting realistic and adaptable UAV simulation:

- Command Flow: QGC sends high-level mission commands to PX4, which PX4 interprets and uses to guide UAV movements within Gazebo.
- Simulation Feedback: Gazebo provides continuous environmental data to PX4, enabling the UAV to adjust its flight dynamics based on simulated terrain and environmental factors.
- Monitoring and Adjustment: QGC receives telemetry updates from PX4, empowering operators to observe UAV performance in real time, make mission adjustments, or override control as needed.

3.2.2. Data generation

The framework generates several sensor measurements that can be used in several algorithmic developments such as visual-inertial odometry, LiDAR-inertial odometry, and trajectory prediction. This comprehensive data generation setup replicates complex terrain and challenging conditions, supporting thorough testing of localization and navigation algorithms in simulated outdoor environments.

We developed a custom ROS 2 tool, **uav_dataset_generation_ros** package [64], to automate and synchronize the creation of comprehensive UAV datasets. This package systematically collects synchronized telemetry and sensor data during each simulated mission, ensuring consistency across all data points. The dataset includes synchronized 3D position trajectories, GPS coordinates, IMU readings, RGB images, LiDAR-based distance measurements, and depth images. The dataset generation process employs simulated UAV missions using two distinct trajectory approaches: user-defined trajectories and parametric trajectories. User-defined trajectories provide precise control over trajectory characteristics, including path length, geometric shape, and coverage of specific regions. However, this approach lacks the automation capabilities required for generating large numbers of random trajectories efficiently.

Parametric trajectories address this limitation by employing mathematical parameterization through control variables that govern trajectory size, velocity profile, radius, and spatial orientation. This parameterization enables the automated generation of an arbitrary number of random trajectories, making it well-suited for large-scale dataset creation. Two parametric trajectory types are implemented: circular and lemniscate (infinity-shaped) trajectories.

A circular trajectory in three-dimensional space is uniquely defined by four fundamental parameters:

- Normal Vector: $\mathbf{n} = \frac{\mathbf{n}_{orig}}{|\mathbf{n}_{orig}|}$, where $\mathbf{n}_{orig}$ is an arbitrary vector normal to the plane containing the circular trajectory with its origin at the circle's 3D center.
- Center Position: $\mathbf{c} \in \mathbb{R}^3$, representing the geometric center of the circle.
- Radius: $r > 0$, defining the circle's radius.
- Angular Velocity: $\omega > 0$, controlling the traversal rate along the trajectory.

The position vector along the circular trajectory at time t is given by Equation (1):

$$\mathbf{p}_c(t) = \mathbf{c} + r \cdot (\cos(\omega t) \cdot \mathbf{v_1} + \sin(\omega t) \cdot \mathbf{v_2}), \tag{1}$$

where $\mathbf{v_1}$ and $\mathbf{v_2}$ are orthonormal basis vectors spanning the plane perpendicular to $\mathbf{n}$.

The lemniscate (infinity-shaped) trajectory employs the same parameterization framework as the circular trajectory but generates a figure-eight pattern through a modified trajectory equation. Using identical definitions for the normal vector, center position, radius, and angular velocity, the lemniscate trajectory position is defined by Equation (2):

$$\mathbf{p}_\infty(t) = \mathbf{c} + r \cdot (\cos(\omega t) \cdot \mathbf{v_1} + \sin(2\omega t) \cdot \mathbf{v_2}). \tag{2}$$

The frequency-doubling factor in the sine component ($2\omega t$) creates the characteristic figure-eight geometry by introducing a 2:1 frequency ratio between the orthogonal motion components.

By executing either user-defined or parametric trajectories, our framework generates timestamped and synchronized measurements that can be used for analysis and algorithmic development. Each UAV simulated trajectory will generate a structured dataset explained as follows.

CSV data structure Each mission's essential UAV and environmental parameters are recorded in a structured CSV file, capturing the following key columns:

- `timestamp`: Precise timestamp for each data entry, ensuring accurate temporal alignment.
- `image_name`: Filename of the captured UAV image at each position, providing a visual reference.
- `tx`, `ty`, `tz`: 3D positional coordinates in the simulated environment.
- `vel_x`, `vel_y`, `vel_z`: UAV velocity along the x, y, and z axes.
- `orientation_x`, `orientation_y`, `orientation_z`: Orientation values representing the UAV's attitude.
- `angular_vel_x`, `angular_vel_y`, `angular_vel_z`: Angular velocity components indicating rotational dynamics.
- `linear_acc_x`, `linear_acc_y`, `linear_acc_z`: Linear acceleration components describing UAV movement behavior.
- `latitude`, `longitude`: GPS coordinates for precise trajectory mapping.
- `lidar_range`: LiDAR sensor measurements.
- `AMSL`: Altitude above mean sea level, valuable for altitude-based analyses.

UAV trajectory and region overview images Trajectory images, captured by the UAV's camera at each recorded position, are stored in the `data_recordings` folder and synchronized with telemetry data to provide a detailed visual perspective of the UAV's environment. These images are essential for testing algorithms reliant on visual input, such as SLAM and visual navigation. Additionally, a lower-resolution PNG image offering a comprehensive view of the entire region is included to aid in general visualization and planning, complementing the high-resolution trajectory images and providing valuable context. This structured dataset supports flexible and thorough analysis, facilitating the testing of localization, navigation, and obstacle avoidance algorithms under realistic conditions.

3.2.3. *Sensor configuration and data collection details*

The OS-RFODG framework is designed with attention to sensor realism, spatial relationships, and data synchronization. Below, we detail the simulated sensor setup, their integration within the UAV frame, and the configuration strategies used to ensure reliable and reproducible dataset generation.

- Simulated Sensor Configuration: The OS-RFODG framework employs accurately modeled virtual sensors within the Gazebo simulation environment, eliminating the need for physical calibration while maintaining realistic sensor characteristics:

- **Camera Sensors**: Simulated RGB cameras are configured with realistic intrinsic parameters including focal length (fx = fy = 277.19), principal point (cx = 160, cy = 120), and image resolution (320×240 pixels). Camera intrinsics are automatically published as ROS2 `sensor_msgs/CameraInfo` messages, which can be used in further image processing.
- **IMU Sensors**: Virtual IMU units simulate 6-DOF motion with configurable noise parameters: accelerometer noise (0.01 m/s^2), gyroscope noise (0.001 rad/s), and bias drift characteristics matching commercial-grade sensors (e.g., MPU-6050 specifications).
- **LiDAR Sensors**: Simulated LiDAR units provide range measurements with specified parameters: range limits (0.1 m to 120 m), angular resolution (0.25°), scan frequency (10 Hz), and Gaussian noise ($\sigma = 0.02$ m) to replicate real-world sensor behavior.
- **GPS Sensors**: Virtual GPS modules generate realistic position estimates with configurable accuracy parameters: horizontal accuracy (±2 m), vertical accuracy (±3 m), and update frequency (5 Hz) matching typical UAV GPS units.
- **Barometer Sensors**: Simulated barometric altimeters provide pressure-based altitude estimates with noise characteristics ($\sigma = 0.1$ m) and temperature-compensation effects.

- Spatial Sensor Relationships and TF Tree: All sensor positions and orientations are precisely defined within the simulated UAV frame and published through ROS 2's Transform (TF) system:

- **TF Tree Structure**: The complete spatial relationship between sensors is maintained in the ROS 2 TF tree with transformations from the UAV base frame to each sensor frame (e.g., `base_link` → `camera_link`, `base_link` → `imu_link`).
- **Sensor Mounting Positions**: A downward-looking camera was mounted at UAV front (translation: [0.1, 0.0, -0.05]m, rotation: [0, 1.5708, 0]rad), IMU at center of mass (translation: [0.0, 0.0, 0.0]m), LiDAR beneath UAV (translation: [0.0, 0.0, -0.1]m), GPS antenna on top (translation: [0.0, 0.0, 0.1]m).
- **Coordinate Frame Consistency**: All sensor measurements are referenced to a common coordinate system with consistent timestamp alignment, eliminating calibration uncertainties present in real hardware systems.

- Data Synchronization Mechanisms: The framework implements precise temporal alignment through ROS 2's real-time infrastructure:

- **Simulation Time Synchronization**: All sensors operate under Gazebo's simulation clock, ensuring perfect temporal alignment across all modalities with microsecond precision timestamps.
- **Message Filtering**: The framework employs ROS 2's `message_filters` library with `ApproximateTime` policy for synchronizing multi-modal sensor streams. Time tolerance is set to 10 ms to

accommodate different sensor publication rates while maintaining temporal coherence.
- **Quality of Service (QoS) Configuration**: Sensor topics use differentiated QoS profiles: `RELIABLE` for GPS and LiDAR data requiring guaranteed delivery, and `BEST_EFFORT` for high-frequency IMU streams (200 Hz) to minimize latency.

- Reproducibility and Configuration Management: To facilitate experimental reproduction, the following standardized procedures and configurations are provided:

- **Environment Setup**: Ubuntu 22.04 LTS with ROS 2 Humble, Gazebo 11.10+, PX4 v1.14+, and QGroundControl v4.2+.
- **Hardware Requirements**: Minimum 16 GB RAM, 8-core CPU, and GPU with 4 GB VRAM for real-time simulation.
- **Sensor Configuration Files**: All Gazebo sensor models, ROS 2 launch files, and parameter configurations are provided in standardized formats (YAML/XML) within the open-source repository.
- **TF Configuration**: Complete TF tree definitions and sensor mounting specifications are included as ROS 2 launch parameters.
- **Data Collection Protocol**: Standardized flight mission templates, trajectory generation scripts, and synchronization configurations ensure consistent experimental conditions across different research groups.

3.2.4. Sensor synchronization and terrain integration details

The OS-RFODG framework ensures accurate multi-sensor data alignment by leveraging ROS 2's real-time communication and clock management infrastructure. All sensor nodes operate under a unified ROS 2 clock and publish data with precise timestamps using high-resolution system timers. Sensor messages (e.g., IMU, GPS, LiDAR, camera) are synchronized through ROS 2 callback queues with deterministic Quality-of-Service (QoS) settings and optional use of message filters or custom synchronizers. This approach guarantees microsecond-level alignment across modalities, crucial for time-dependent fusion algorithms. Additionally, the terrain modeling process is modular and reproducible: high-resolution GeoTIFF files (DEM, DSM, DTM) are processed in QGIS and exported with accurate spatial referencing. These elevation maps are converted into textured 3D meshes in Blender using the displacement modifier and UV mapping techniques to preserve real-world topography. The resulting terrain models are integrated into the Gazebo simulation environment via Collada (.dae) files with embedded texture and heightmap data. This end-to-end pipeline enables researchers to generate geographically grounded UAV datasets with consistent spatial and temporal accuracy, supporting rigorous benchmarking of terrain-aware localization systems.

Our sensor synchronization module uses ROS 2's `message_filters` library with the ApproximateTime policy, which balances temporal alignment across modalities sampled at different rates. Sensor nodes are configured using the SensorData QoS profile with `BestEffort` reliability for high-frequency data (e.g., IMU) and `Reliable` settings for positional sources (e.g., GPS, LiDAR). This configuration minimizes latency while ensuring robustness during fusion tasks. To the best of our knowledge, OS-RFODG is the first open-source UAV dataset framework that integrates QGIS-derived elevation maps, ROS 2-native synchronization, and Gazebo-based terrain simulation in a modular ROS 2 pipeline.

4. Implementation and results

This section evaluates the effectiveness of the OS-RFODG framework in generating precise UAV localization datasets, utilizing metrics including elevation error, trajectory alignment, and the accurate localization of UAV-captured images across the entire map.

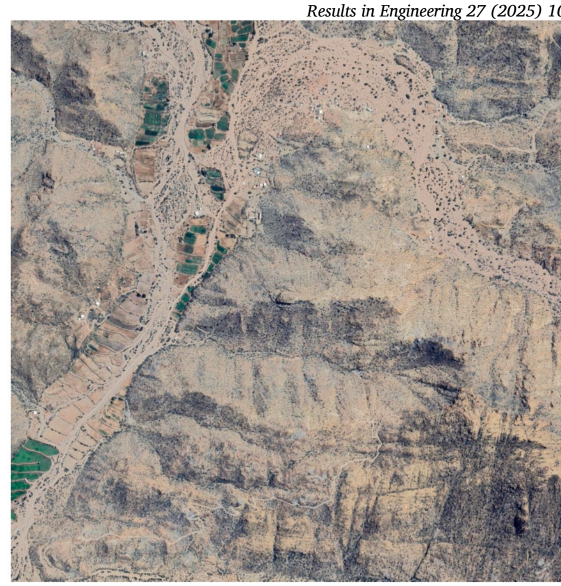

Fig. 2. Satellite view of a part of the Makkah Region, Saudi Arabia.

Table 3
Geospatial attributes and metadata corresponding to the Taif region.

Attribute	Value
File Name	Makkah.tif
Width (pixels)	415
Height (pixels)	155
Coordinate Reference System	EPSG:4326
Resolution (degrees/pixel)	0.000277778
Resolution (meters/pixel)	$\approx$ 28.81
Bounding Box (Min Longitude, Min Latitude)	(40.1671, 21.3076)
Width (km)	$\approx$ 11.41
Height (km)	$\approx$ 5.01
Surface Area (km^2)	$\approx$ 57.93

4.1. Region selection

The Makkah Region in Saudi Arabia, as illustrated in Fig. 2, was selected for generating datasets for UAV flights using our OS-RFODG framework. This region's diverse topographical features make it an ideal setting for evaluating the performance of our open-source framework (see Table 3). The corner point of this region is located at $21^\circ 16' 50''$N latitude and $40^\circ 13' 06''$E longitude, with an elevation of 847.25 m. This area represents a typical mountainous and desert environment of Saudi Arabia, combining a few urban elements, such as houses, hospitals, and mosques, along with extensive rural landscapes and mountainous terrains. As illustrated in Fig. 3, the generated datasets comprise both 2D and 3D representations, including DEMs and DSMs, which support detailed terrain analysis and capture the region's complex topography. In the selected region, we identify the following key features:

- **Rural Landscapes:** Open spaces crucial for testing long-range UAV flights and ensuring sensor accuracy over large areas.
- **Mountainous Terrain:** Diverse elevations and complex topographical features that enable thorough assessment of UAV performance.

4.2. UAV trajectory and dataset generation

The OS-RFODG framework employs advanced simulation tools, including Gazebo and PX4, to capture comprehensive sensor measurements during UAV flights. The following key sensors were integrated into the UAV throughout these simulations:

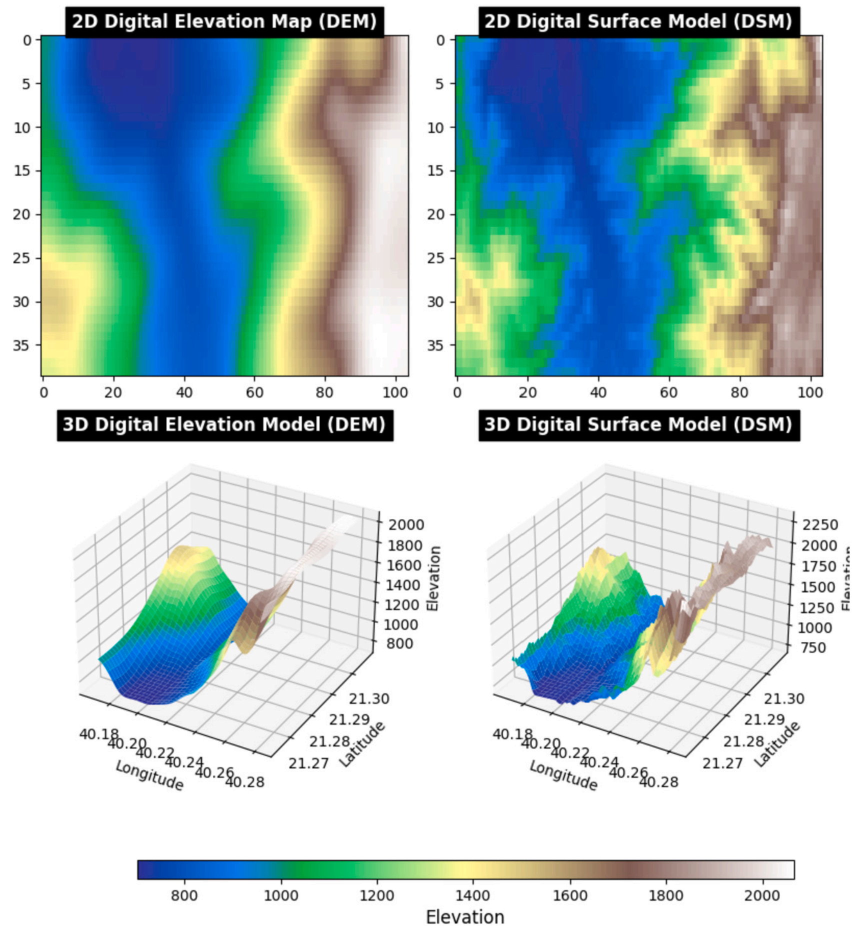

Fig. 3. 2D and 3D Representations of the Makkah Region: DEM and DSM.

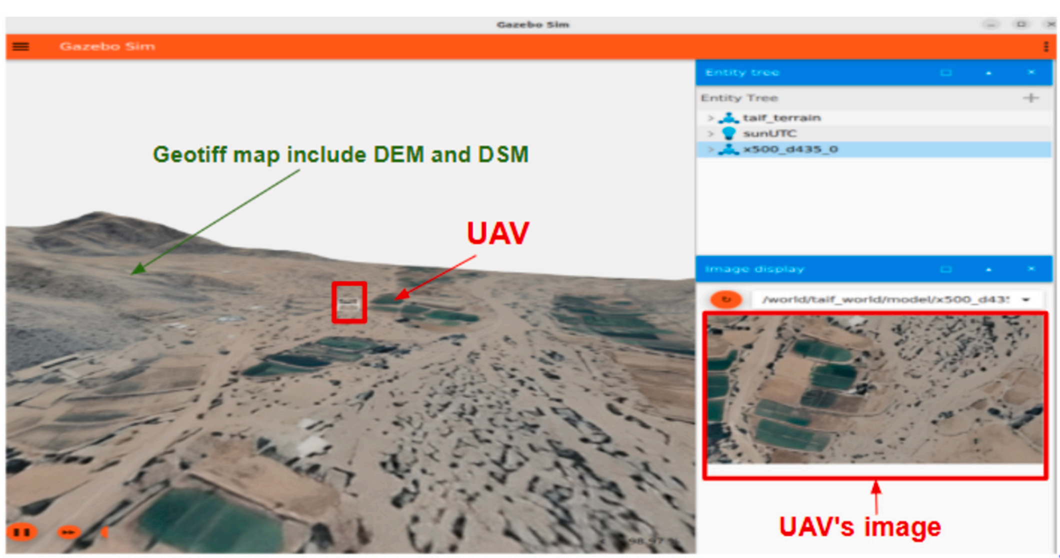

Fig. 4. A snapshot of the Gazebo simulator showing the simulated drone in a digital elevation and surface maps (left), with a stream of the drone's onboard camera sensor (right).

- **LiDAR**: Provides distance measurements essential for mapping terrain features and detecting obstacles.
- **GPS**: Supplied positional data, including latitude and longitude.
- **IMU**: Recorded orientation, acceleration, and angular velocity for motion tracking.
- **Barometer**: Measures atmospheric pressure to determine altitude above sea level, providing accurate elevation data for UAV flight stability and height correction.
- **Camera**: Captures visual data in `.png` format with RGB color channels (see Fig. 4).

Fig. 5. User-defined UAV trajectory in QGroundControl software.

Table 4
Data size, distance, and elevation measurements for various datasets.

Trajectory	Data Size (data points)	Distance (km)	Min Real Elevation (m)	Max Real Elevation (m)
Trajectory 1 (Data 1)	18207	12.2386	759	1007
Trajectory 2 (Data 2)	3708	3.2330	776	1005
Trajectory 3 (Data 3)	21909	14.6971	750	979
Trajectory 4 (Data 4)	18004	11.5876	754	1039
Trajectory 5 (Data 5)	13861	9.3097	754	884
Trajectory 6 (Data 6)	10396	6.9381	750	894

The OS-RFODG framework was evaluated by generating six user-defined distinct trajectories using waypoints in QGC, as illustrated in Fig. 5, and comparing them to real-world data to assess accuracy. Data collected from these flights included measurements from key sensors, enabling comprehensive performance analysis.

The flexibility in selecting trajectories allows for exploration across multiple scenarios, providing valuable insights into the capabilities of the OS-RFODG framework.

Each flight's data was saved as an individual dataset, labeled Data 1 through Data 6 (see Table 4), containing positional, sensor, and elevation information from the UAV's onboard systems. The corresponding flight distances range from approximately 3.23 km to 14.70 km, reflecting diverse mission lengths and complexities. These datasets capture a broad range of terrain types, flight patterns, and environmental conditions, making them well-suited for extensive testing and evaluation. This diverse collection enhances the framework's versatility, providing a robust foundation for benchmarking UAV localization methods across varied topographies and operational scenarios.

Among the generated datasets, Trajectory 3 (Data 3) stands out with the largest number of data points, totaling 21,909, while Trajectory 2 (Data 2) has the fewest, with only 3,708 data points. In terms of elevation metrics, Trajectory 4 (Data 4) reaches the highest maximum elevation of 1,039 meters, whereas Trajectory 6 (Data 6) records the lowest maximum elevation at 894 meters. The absolute elevation variations across the trajectories indicate significant differences. Trajectory 1 (Data 1) exhibits an elevation range of 248 meters, with values spanning from 759 to 1,007 meters. Trajectory 2 (Data 2) and Trajectory 3 (Data 3) both show a variation of 229 meters. In contrast, Trajectory 4 (Data 4) demonstrates the most substantial variation at 285 meters, ranging from 754 to 1,039 meters.

Trajectory 5 (Data 5) presents a more constrained range of 130 meters, while Trajectory 6 (Data 6) reflects a variation of 144 meters. These differences underscore the diverse topographical challenges associated with each trajectory, which are critical for evaluating the efficacy of UAV localization methodologies.

4.3. *Performance metrics*

In this study, the performance of the OS-RFODG framework is assessed using three key metrics: trajectory alignment, elevation accuracy, and visual consistency. Trajectory alignment is verified by comparing the world-coordinate positions saved by the framework during simulation with the predefined routes from QGroundControl, visualized in QGIS. Elevation accuracy is evaluated using RMSE between simulated and ground-truth elevation from GeoTIFF data. Visual consistency is validated using SIFT-based image matching to ensure spatial coherence of UAV-captured images for vision-based localization methods.

4.3.1. *UAV trajectory alignment*

UAV trajectory alignment is assessed by exporting the recorded world-coordinate positions from the OS-RFODG framework as KML files and visualizing them in QGIS. Fig. 6 displays the simulated trajectory in QGIS (a) alongside the predefined mission path from QGroundControl (b). These trajectories are plotted using the same geographic reference system, ensuring a direct spatial comparison. The close correspondence between the two trajectories confirms the framework's capability to accurately reproduce planned flight paths within a geospatial simulation environment. This validation step ensures positional consistency and supports the reliable evaluation of localization methods. Moreover, trajectory visualization in QGIS enables analysis of terrain effects on UAV

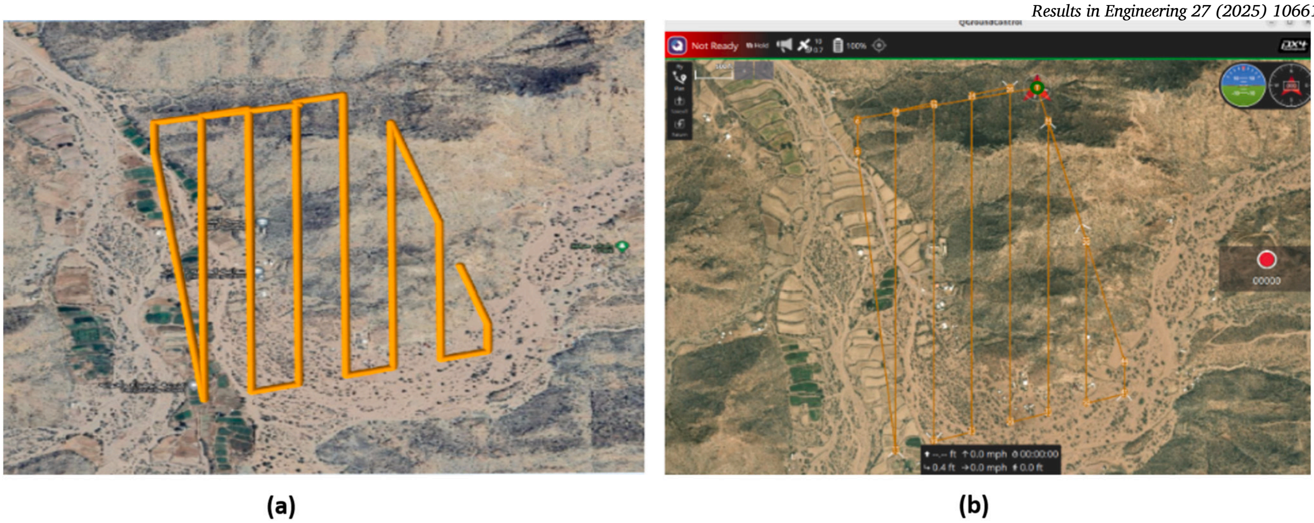

Fig. 6. Comparison of UAV trajectory recorded by the OS-RFODG framework and visualized in QGIS (a) with the corresponding predefined trajectory from QGroundControl (b).

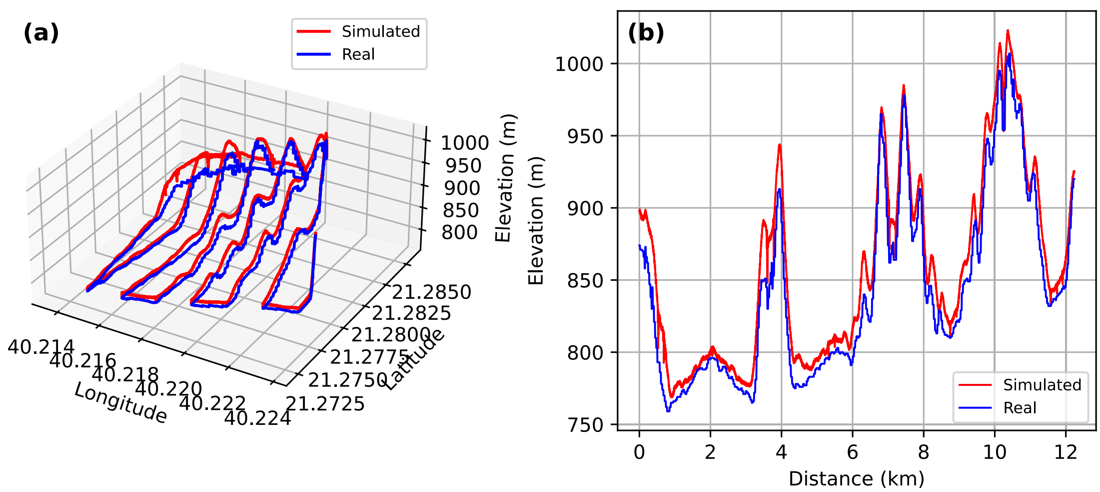

Fig. 7. Trajectory 1: (a) 3D representation of real and framework trajectories in coordinate space, and (b) comparison of elevation profiles between real data and framework predictions.

motion and aids in developing terrain-aware navigation algorithms. This alignment further highlights the practical utility of OS-RFODG in generating datasets that are both spatially coherent and suitable for evaluating GNSS-denied navigation solutions.

4.3.2. Elevation metric error

The OS-RFODG framework demonstrates robust terrain-aware modeling capabilities, with accurate elevation profile reproduction verified across six real-world UAV trajectories (Figs. 7–12). Each figure presents a two-panel view: (a) a 3D overlay of the simulated (red) and real (blue) flight paths in geographic space, and (b) the corresponding elevation profile, plotting elevation against cumulative distance. The close correspondence between the simulated and actual elevation data, in both spatial trajectory and elevation trends, demonstrates the OS-RFODG framework's capability to accurately reconstruct the key topographical features of the Makkah Region. This strong agreement validates OS-RFODG as a dependable tool for generating high-fidelity UAV simulation datasets in complex environments.

As illustrated in Fig. 13, the Root Mean Square Error (RMSE) values across the six UAV trajectories range from 13.59 to 19.5 meters. These results reflect varying levels of accuracy achieved by the OS-RFODG framework in reproducing the real elevation profiles. The average RMSE across all trajectories is approximately 17.86 meters, indicating a reasonable correspondence between the simulated and real-world elevation data.

Trajectory 4 shows the lowest RMSE value (13.59 meters), suggesting limited terrain variability along this path, which facilitates higher simulation accuracy. On the other hand, Trajectory 3 presents the highest RMSE (19.5 meters), likely due to more abrupt elevation changes that introduce complexity in modeling and increase the potential for deviation.

The relatively high RMSE values reported for Trajectories 1, 2, and 5 (ranging from 17.24 to 19.15 meters) underscore the sensitivity of elevation reconstruction to terrain complexity, including gradients, ridges, and sudden altitude shifts. The variation in RMSE across trajectories highlights the influence of terrain complexity on the performance of simulation-based elevation estimation. Despite these challenges, the OS-RFODG framework consistently maintains a high degree of agreement with the actual elevation data. This reinforces its reliability as a tool for generating georeferenced datasets suitable for developing and evaluating UAV localization algorithms in GNSS-denied environments.

To further quantify the precision of the simulated elevation data, we evaluated the Mean Absolute Error (MAE) and Mean Absolute Percentage Error (MAPE) across all six trajectories. As reported in Table 5, Trajectories 4 and 6 yielded the lowest MAE values (11.39 meters and

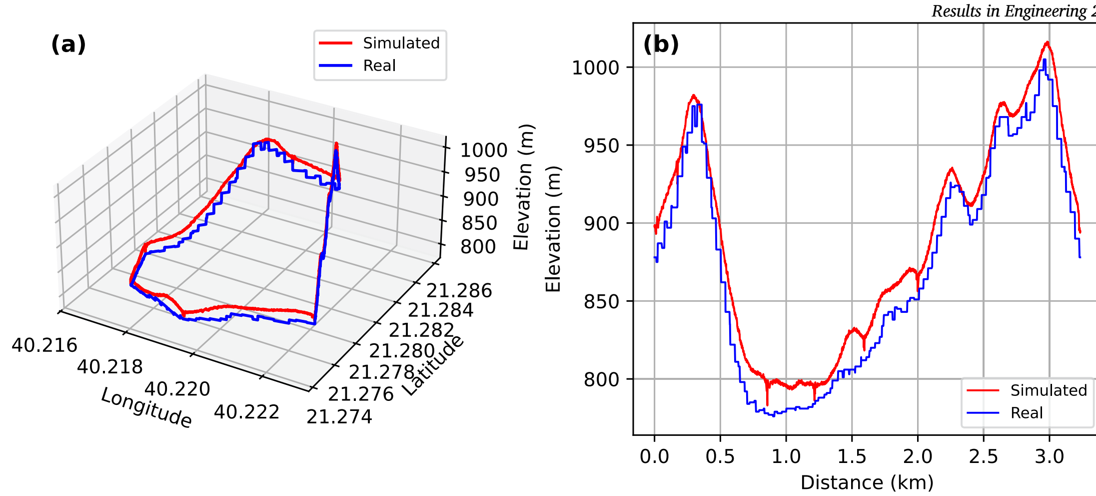

Fig. 8. Trajectory 2: (a) 3D representation of real and framework trajectories in coordinate space, and (b) comparison of elevation profiles between real data and framework predictions.

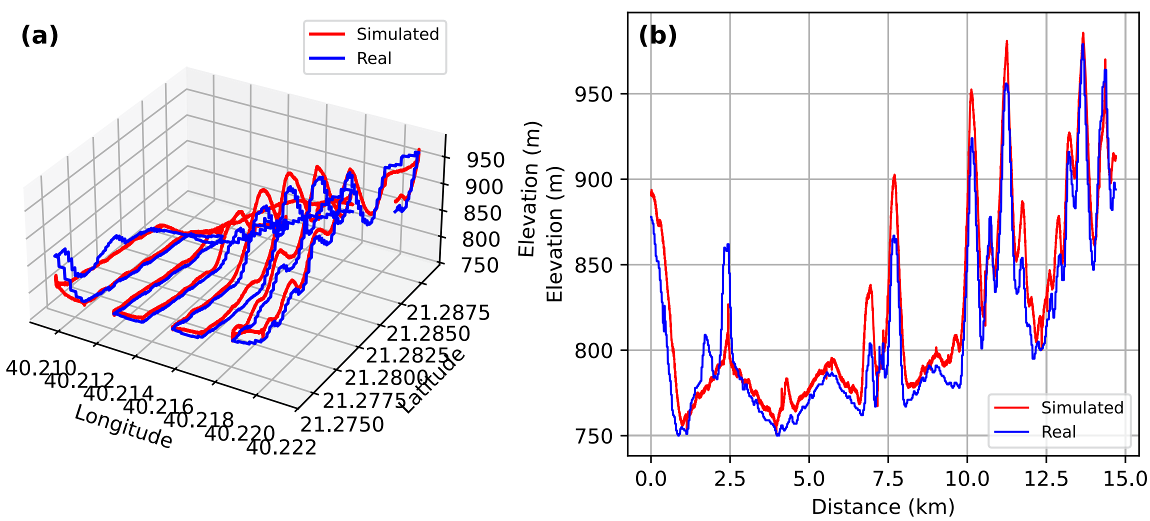

Fig. 9. Trajectory 3: (a) 3D representation of real and framework trajectories in coordinate space, and (b) comparison of elevation profiles between real data and framework predictions.

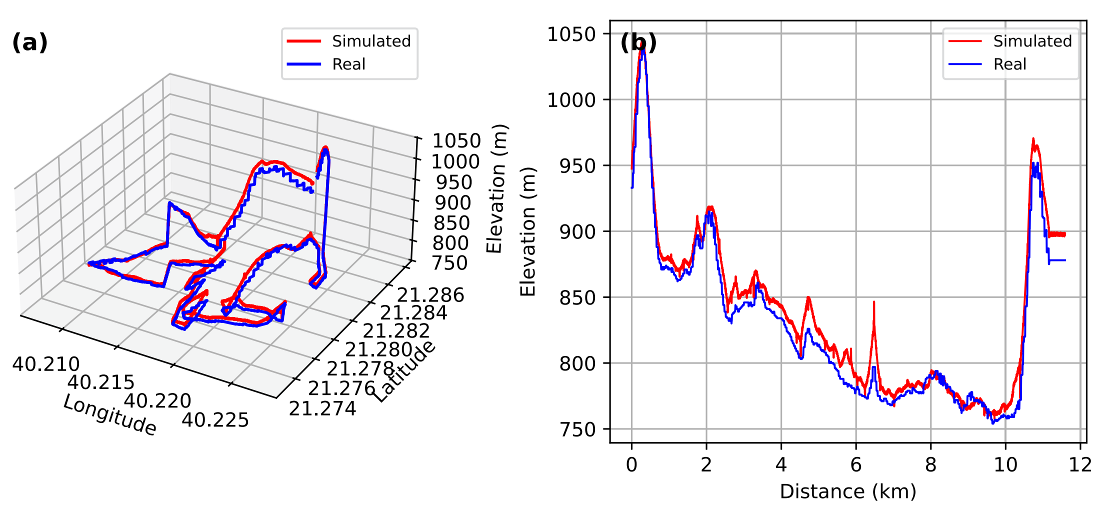

Fig. 10. Trajectory 4: (a) 3D representation of real and framework trajectories in coordinate space, and (b) comparison of elevation profiles between real data and framework predictions.

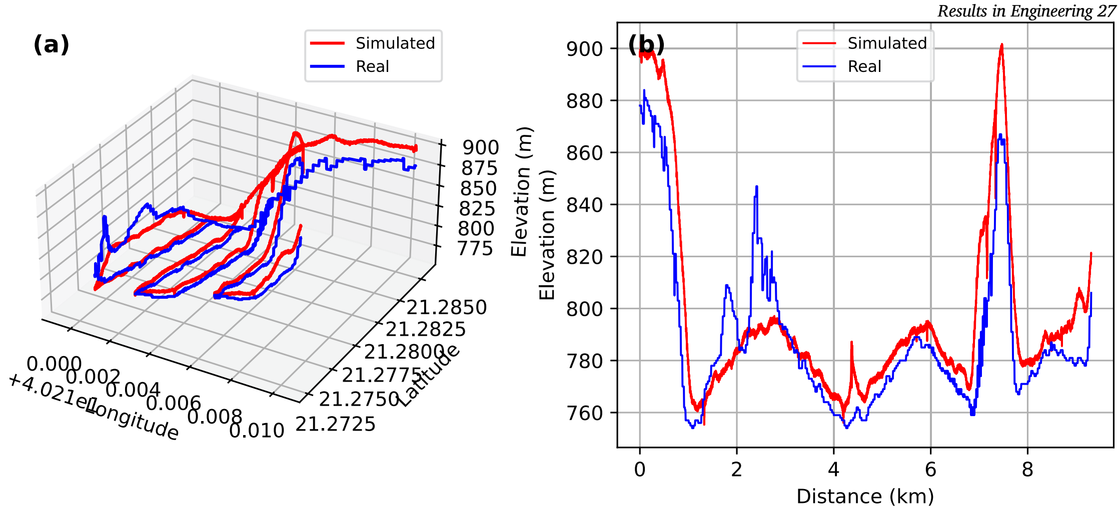

Fig. 11. Trajectory 5: (a) 3D representation of real and framework trajectories in coordinate space, and (b) comparison of elevation profiles between real data and framework predictions.

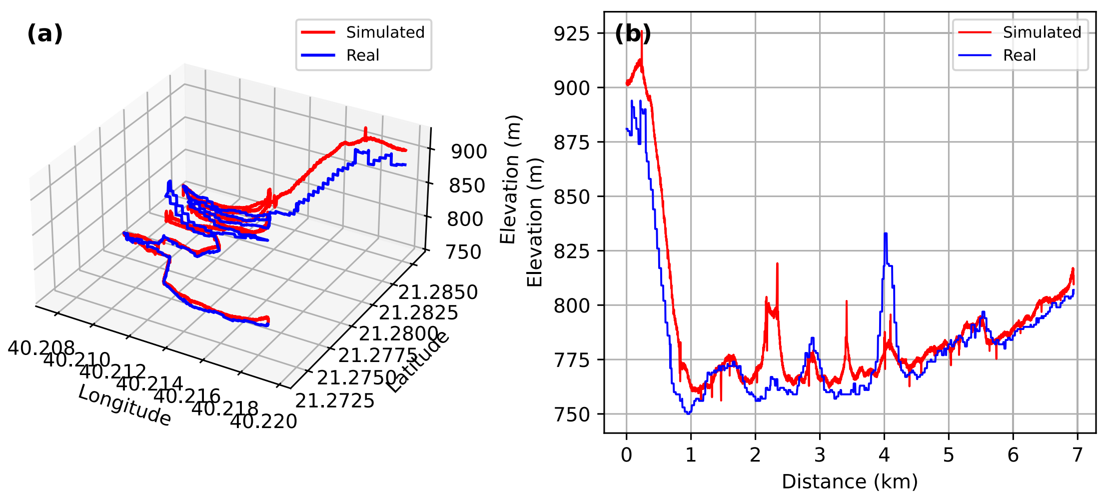

Fig. 12. Trajectory 6: (a) 3D representation of real and framework trajectories in coordinate space, and (b) comparison of elevation profiles between real data and framework predictions.

10.70 meters respectively), indicating consistently small deviations from ground-truth elevation values.

Additionally, MAPE values for these trajectories are below 1.4 percent, highlighting excellent relative accuracy despite absolute elevation shifts. Conversely, the highest MAE value of 16.06 meters was observed for Trajectory 1, aligned with its higher RMSE.

Nonetheless, all MAPE values remain under 2 percent, underscoring the framework's robustness across diverse terrain conditions.

The variation in RMSE, MAE, and MAPE across trajectories highlights the influence of terrain complexity on the performance of simulation-based elevation estimation. Despite these challenges, the OS-RFODG framework consistently maintains a high degree of agreement with the actual elevation data. This reinforces its reliability as a tool for generating georeferenced datasets suitable for developing and evaluating UAV localization algorithms in GNSS-denied environments.

The variation in RMSE, MAE, and MAPE across trajectories highlights the influence of terrain complexity on the performance of simulation-based elevation estimation. Despite these challenges, the OS-RFODG framework consistently maintains a high degree of agreement with the actual elevation data.

This consistent alignment with ground-truth elevation measurements underscores the robustness of the OS-RFODG framework and affirms its reliability in generating georeferenced datasets. The low error margins across multiple trajectories, as indicated by RMSE, MAE, and MAPE metrics, demonstrate the framework's capacity to maintain topographic fidelity even in complex terrain. These accurate elevation reconstructions enable more realistic simulation environments, which

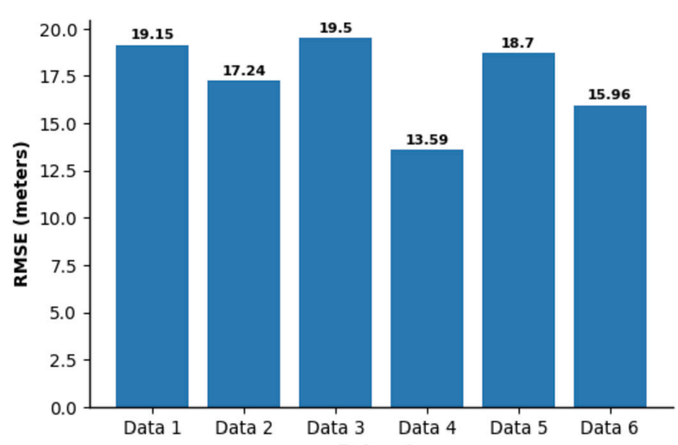

Fig. 13. RMSE comparison of elevation error.

Table 5
Summary of flight statistics for all trajectories, including distance, elevation range, RMSE, MAE, and MAPE.

Trajectory	Distance (km)	Elevation Range (m)	RMSE (m)	MAE (m)	MAPE
Trajectory 1	12.24	248 (759→1 007)	19.15	16.06	0.0190
Trajectory 2	3.23	229 (776→1 005)	17.24	15.99	0.0186
Trajectory 3	14.70	229 (750→979)	19.50	15.42	0.0188
Trajectory 4	11.59	285 (754→1 039)	13.59	11.39	0.0137
Trajectory 5	9.31	130 (754→884)	18.70	14.04	0.0175
Trajectory 6	6.94	144 (750→894)	15.96	10.70	0.0135

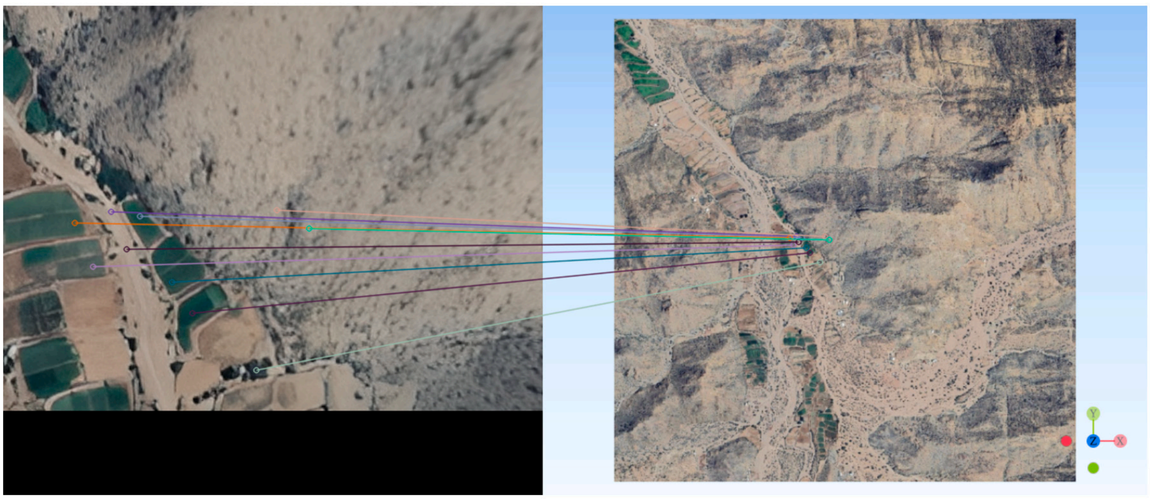

Fig. 14. SIFT-based visual feature correspondences between a UAV-captured image (left) and a georeferenced satellite map of the Taif region (right), centered at coordinates 21.2863825° latitude and 40.2243424° longitude.

are critical for benchmarking and improving UAV navigation and localization techniques. Consequently, the OS-RFODG-generated datasets provide a sound foundation for advancing state-of-the-art solutions in GNSS-denied scenarios, facilitating both algorithmic validation and comparative performance assessment under realistic operational constraints.

4.3.3. Validation of UAV image capture accuracy

This section validates whether UAV-captured images generated by our framework correspond to the correct zones on the map. The Scale-Invariant Feature Transform (SIFT) algorithm is used to match keypoints in UAV images with those in map images, confirming their spatial alignment.

The results, visualized in Figs. 14 and 15, demonstrate that UAV images align accurately with the intended map regions, verifying the framework's precision in capturing the correct areas.

Table 6 presents the precision of the matching process along with root mean square error (RMSE) values in meters for the X (longitude) and Y (latitude) directions. The precision values range between 0.7032 and 0.8964, indicating a high level of keypoint matching accuracy across all locations. RMSE values for X and Y displacements in meters show low error margins, with the maximum RMSE X observed at 1.34 m and RMSE Y at 0.95 m. These results confirm that the framework provides accurate localization of UAV-captured images within the mapped environment.

Analyzing the results, the highest precision (0.8964) is observed for locations 21.2872659°, 40.2207371° and 21.2785681°, 40.2128509°, with relatively low RMSE values, reflecting minimal spatial misalignment.

Conversely, the lowest precision (0.7032) is recorded at 21.2863825°, 40.2243424°, which also corresponds to the highest RMSE values (1.34 m in X and 0.95 m in Y). This suggests that this location posed more significant challenges due to potential variations in elevation or image features.

Table 6
Precision and RMSE metrics for UAV and map image alignment using SIFT.

Location (Latitude, Longitude)	Precision	RMSE X (m)	RMSE Y (m)
21.2863825°, 40.2243424°	0.7032	1.34	0.95
21.2880168°, 40.2205900°	0.8689	1.10	0.83
21.2872659°, 40.2207371°	0.8964	1.07	0.77
21.2785681°, 40.2128509°	0.8964	1.22	0.88

Overall, the combined metrics demonstrate that the framework achieves reliable UAV image alignment across diverse geographic locations, with performance variations largely attributable to environmental factors such as elevation changes and feature density.

The OS-RFODG framework provides the following contributions:

- **Complete and extensible toolchain for terrain-aware UAV simulation:** OS-RFODG integrates a comprehensive set of open-source tools, including QGIS, Blender, ROS 2, Gazebo, PX4, and QGroundControl, into a unified workflow. This combination enables users to create UAV simulation environments that reflect real-world terrain by importing high-resolution elevation data and satellite imagery. Such a configuration is not commonly available in existing public frameworks for UAV dataset generation.
- **Support for terrain-aided localization through integrated altitude sensing and digital elevation maps:** Unlike many existing UAV datasets that either omit terrain data or lack altitude-measuring sensors, OS-RFODG provides synchronized access to both. The dataset includes high-resolution elevation layers (DEM, DSM, and DTM) as well as measurements from sensors such as barometers and LiDAR, which estimate altitude. This dual availability enables researchers to apply terrain-matching techniques that compare onboard altitude readings to known terrain profiles. The

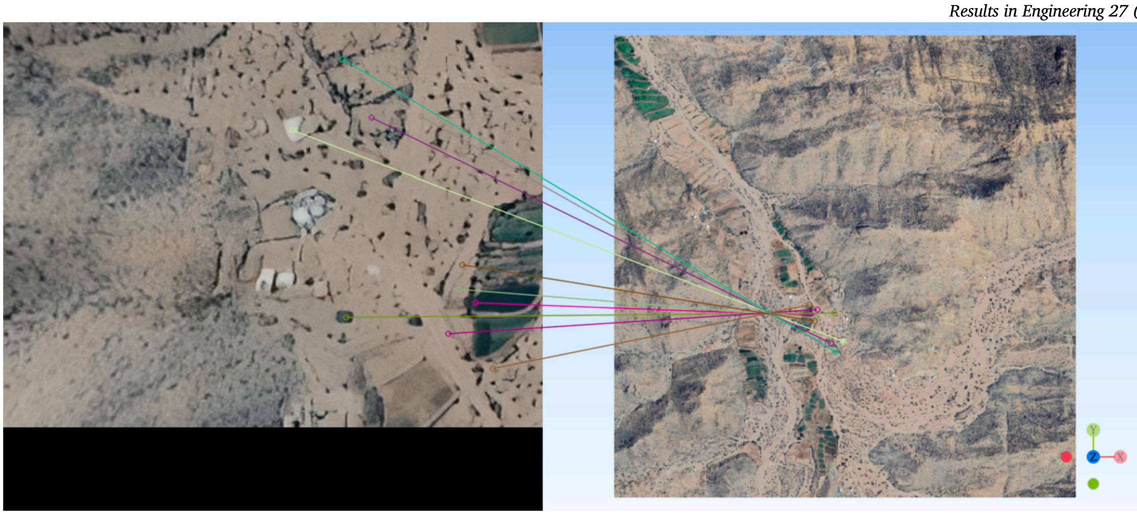

Fig. 15. SIFT-based feature correspondences between the UAV-captured image (left) and the georeferenced satellite map (right) of the Taif region, centered at coordinates 21.2880168° latitude and 40.22059° longitude.

inclusion of both sources is essential for evaluating terrain-aided navigation algorithms, especially under GNSS-denied conditions.

- **Multi-sensor, time-synchronized data generation:** The framework allows the collection of structured data from multiple sensors, including RGB cameras, LiDAR, IMU, barometers, and GNSS receivers. All data streams are precisely synchronized using ROS 2 middleware. This capability is essential for evaluating sensor fusion algorithms that require consistent timestamp alignment between modalities.
- **Customizable mission planning based on terrain context:** Through the integration with PX4 and QGroundControl, the framework supports the creation of customized flight missions that adapt to elevation data. This allows for simulating realistic UAV operations over topographically diverse areas and enables the testing of terrain-aware navigation strategies.
- **Structured and reproducible data output for benchmarking:** The framework produces standardized outputs in CSV and image formats that include sensor readings, geospatial references, and ground-truth elevation. These outputs are designed to support benchmarking of visual-based, sensor fusion, and learning-based localization methods under degraded or denied GNSS conditions.

4.3.4. *Comparison with existing real-flight UAV datasets*

Direct comparisons between UAV datasets can be challenging due to differing objectives, sensor setups, geographic coverage, and evaluation metrics. Nevertheless, it remains valuable to examine key aspects across representative works to contextualize dataset design choices and contributions. Table 7 presents a structured comparison of five prominent real-flight UAV datasets: UAVD4L [47], VDUAV [48], University-1652 [55], INSANE [11], and UAV-VisLoc [17] highlighting differences in sensor modalities, elevation data availability, synchronization approaches, and localization accuracy. This comparison provides a basis for understanding the evolving landscape of UAV dataset development and for situating the contributions of the OS-RFODG framework.

Unlike most existing real-flight UAV datasets, OS-RFODG integrates a comprehensive set of visual and non-visual sensors, including RGB cameras, LiDAR, IMU, GNSS, and barometric sensors, alongside detailed geospatial elevation layers such as DEM, DSM, and DTM. This multimodal configuration enables accurate 3D localization, achieving an RMSE of 1.19 m in longitude and 0.86 m in latitude. These results demonstrate the dataset's suitability for evaluating localization algorithms in GNSS-degraded or terrain-constrained environments.

In contrast, many benchmark datasets such as UAV-VisLoc, VDUAV, and University-1652 focus exclusively on visual matching tasks using RGB imagery and do not include elevation maps or inertial measurements. This limits their applicability in terrain-aware or GNSS-denied environments. The UAVD4L dataset includes a DSM and textured 3D model, but it primarily addresses synthetic-to-real image alignment with less emphasis on sensor diversity. The INSANE dataset provides high-precision ground truth based on advanced instrumentation but lacks terrain elevation data, which restricts its use in terrain-aided navigation applications.

Overall, OS-RFODG provides a structured and well-documented dataset that includes synchronized visual and non-visual sensor data along with georeferenced elevation layers. These features support the development and evaluation of advanced sensor fusion techniques, machine learning models, and terrain-aided localization strategies. The dataset is particularly useful for UAV navigation in complex environments where GNSS signals are limited or unavailable, enabling researchers to design and benchmark robust localization pipelines under realistic operating conditions.

In summary, this comparative analysis underscores the advantages of OS-RFODG in relation to existing real-flight UAV datasets. Whereas most benchmark datasets concentrate solely on visual matching tasks and often omit elevation or inertial measurements, OS-RFODG offers a multimodal, time-synchronized dataset enriched with high-resolution DEM, DSM, and DTM layers. As summarized in Table 7, the integration of both visual and non-visual sensors, alongside detailed terrain context, enables accurate localization performance with RMSE values approaching one meter. These characteristics establish OS-RFODG as a comprehensive resource for the development and evaluation of terrain-aware localization techniques, particularly in environments where GNSS signals are unreliable or unavailable. This addresses notable gaps in prior datasets and enhances the applicability of the framework for advanced UAV navigation research.

4.4. *Limitations and challenges*

The open-source OS-RFODG framework accurately replicates real-world conditions, providing essential data for developing, training, and testing localization algorithms in complex outdoor environments. Despite its versatility for UAV dataset generation and simulation, the framework has certain limitations.

One notable constraint is the fixed resolution of DEM used within the framework; currently, a 28-meter GeoTIFF resolution is standard, which may limit terrain detail in high-precision applications. The framework also lacks support for dynamic environmental factors, such as variable

Table 7
Comparison of OS-RFODG with recent real-flight UAV datasets.

Dataset	Visual sensors	Additional sensors	Elevation layer	Primary metric (as published)
UAVD4L [47]	RGB, Depth	IMU, RTK-GPS	DSM, Textured 3D Model	96.68% of images localized within 5 m and 5° orientation error
VDUAV [48]	RGB (drone, satellite)	None	None	MA@5: 45.13%, MA@10: 64.72%, MA@20: 83.35%; RDS: 74.13%
University-1652 [55]	RGB (drone, satellite)	None	None	Recall@1: 65.34% (Drone→Satellite); mAP: 49.78%
INSANE [11]	Stereo, Mono RGB	Triple IMU, Dual RTK-GNSS, UWB, LiDAR, Barometer	None	Ground-truth accuracy < 0.01 m (position), < 0.1° (orientation), 1σ level
UAV-VisLoc [17]	RGB	None	None	Satellite resolution: 0.3 m/pixel; image resolution: 0.1–0.2 m/pixel
OS-RFODG (ours)	RGB	LiDAR, IMU, GPS, Barometer	DEM, DSM, DTM	RMSE(longitude, latitude): 1.19 m, 0.86 m;

weather, wind, and moving obstacles, which impact the realism of adaptive scenarios. Additionally, while OS-RFODG efficiently synchronizes multi-sensor data, it does not yet support advanced sensor fusion capabilities to fully integrate diverse inputs (e.g., LiDAR, IMU, GPS), which could enhance situational awareness and data reliability.

The reliance on 3D terrain modeling and multi-sensor integration imposes substantial computational demands, potentially limiting scalability for users with constrained processing resources. These limitations highlight key areas for future enhancements, positioning OS-RFODG to evolve into an even more comprehensive tool for UAV research, suited to increasingly complex and dynamic simulation environments.

Future work will extend OS-RFODG along several dimensions. Planned improvements include the incorporation of additional sensor modalities such as radar and thermal cameras, the simulation of dynamic environments with moving obstacles and variable weather, and the integration of real-time AI decision-making loops. Furthermore, the framework will be expanded to support benchmarking pipelines for evaluating localization and SLAM algorithms under diverse terrain and visibility conditions. These enhancements are expected to significantly improve the robustness and applicability of UAV localization and navigation research. By enabling comprehensive testing in highly dynamic and GNSS-denied environments, OS-RFODG will better support the development of advanced sensor-fusion and terrain-aware algorithms for critical UAV missions such as search and rescue, surveillance, and environmental monitoring. All components will remain open-source to enhance collaborative development and encourage adoption by the wider robotics and geospatial research communities.

5. Conclusion

This paper introduced OS-RFODG, an open-source framework developed on the Robot Operating System 2, designed to support the generation of high-fidelity, multi-sensor datasets for outdoor unmanned aerial vehicle localization. The framework integrates terrain modeling using QGIS and Blender, flight simulation via PX4 and Gazebo, and microsecond-level synchronized sensor data streaming through ROS 2. It supports both visual and non-visual sensing modalities, including RGB camera, LiDAR, inertial measurement unit, and barometric altimeter. Experimental validation demonstrates that simulated elevation profiles achieve a RMSE below 19 meters when compared to real terrain models. Moreover, the localization accuracy in horizontal coordinates achieved an average RMSE of approximately 1.19 meters in longitude and 0.86 meters in latitude. The framework also enables terrain-aware mission planning through QGroundControl, allowing the generation of flight paths adapted to varied topographies. Each dataset includes structured outputs in CSV and image formats, providing time-synchronized and georeferenced measurements such as position, velocity, acceleration, orientation, barometric altitude, LiDAR range, and camera imagery. One of the key contributions of OS-RFODG is its capacity to support terrain-aided localization methods. By integrating both digital maps (DEM, DSM, and DTM) and sensor-based altitude measurements from barometers and LiDAR, it enables the evaluation of algorithms that match terrain profiles to onboard data. This capability is especially valuable for advancing localization techniques in outdoor scenarios where GNSS signals are degraded or entirely unavailable. Future work will extend OS-RFODG along several dimensions. Planned improvements include the incorporation of additional sensor modalities such as radar and thermal cameras, the simulation of dynamic environments with moving obstacles and variable weather, and the integration of real-time AI decision-making loops. Furthermore, the framework will be expanded to support benchmarking pipelines for evaluating localization and SLAM algorithms under diverse terrain and visibility conditions. These enhancements are expected to significantly improve the robustness and applicability of UAV localization and navigation research. By enabling comprehensive testing in highly dynamic and GNSS-denied environments, OS-RFODG will better support the development of advanced sensor-fusion and terrain-aware algorithms for critical UAV missions such as search and rescue, surveillance, and environmental monitoring. All components will remain open-source to enhance collaborative development and encourage adoption by the wider robotics and geospatial research communities.

CRediT authorship contribution statement

Imen Jarraya: Writing – original draft, Software, Methodology. **Mohamed Abdelkader:** Writing – original draft, Software, Methodology, Investigation. **Khaled Gabr:** Visualization, Validation, Software. **Muhammad Bilal Kadri:** Writing – review & editing, Funding acquisition, Formal analysis. **Fatimah Alahmed:** Writing – original draft, Validation, Methodology, Data curation, Conceptualization. **Wadii Boulila:** Writing – review & editing, Supervision, Project administration, Methodology, Investigation. **Anis Koubaa:** Writing – review & editing, Project administration, Methodology, Investigation, Funding acquisition.

Declaration of competing interest

The authors declare that they have no known competing financial interests or personal relationships that could have appeared to influence the work reported in this paper.

Acknowledgements

The authors extend their sincere appreciation to Prince Sultan University for covering the Article Processing Charges (APC) associated with this publication.

Data availability

The data that has been used is confidential.

References

[1] Abdennabi Morchid, Rachid Jebabra, Abdulla Ismail, Haris M. Khalid, Rachid El Alami, Hassan Qjidaa, Mohammed Ouazzani Jamil, IoT-enabled fire detection for

sustainable agriculture: A real-time system using flask and embedded technologies, Results Eng. 23 (2024) 102705.

[2] Abdennabi Morchid, Rachid Jebabra, Hassan Qjidaa, Rachid El Alami, Mohammed Ouazzani Jamil, Agri-tech innovations for sustainability: A fire detection system based on mqtt broker and iot to improve environmental risk management, Results Eng. 24 (2024) 103683.

[3] Abdul Aabid, Bisma Parveez, Nagma Parveen, Sher Afghan Khan, Omar Shabbir, A case study of unmanned aerial vehicle (drone) technology and its applications in the covid-19 pandemic, J. Mech. Eng. Res. Dev. 45 (2) (2022) 70–77.

[4] Muhammad Junaid, M.E. Al-Atroush, Sajid Mahmood, Kausar Sultan Shah, Arshad Ullah, Recent developments in unmanned aerial vehicle (uav) surveys for rock slope stability analysis—a review, Geocarto Int. 40 (1) (2025) 2519915.

[5] Bin Fang, Zhiwei Zhong, Xiangjun Jiang, A high accuracy and large-scale detection for fixed-wing uav autonomous ground landing with gnss-denied, IEEE Access (2025).

[6] Peng Chen, Xinyu Zhao, Lina Zeng, Luxinyu Liu, Shengjie Liu, Li Sun, Zaijin Li, Hao Chen, Guojun Liu, Zhongliang Qiao, et al., A review of research on slam technology based on the fusion of lidar and vision, Sensors 25 (5) (2025) 1447.

[7] Md. Touhidul Islam, Keisuke Yoshida, Satoshi Nishiyama, Koichi Sakai, Mutual validation of remote hydraulic estimates and flow model simulations using uav-borne lidar and deep learning-based imaging techniques, Results Eng. 20 (2023) 101415.

[8] Tuan Li, Xiaoyang Yu, Qiufang Lin, Yuezu Lv, Guanghui Wen, Chuang Shi, Distributed cooperative localization for unmanned systems using uwb/ins integration in gnss-denied environments, IEEE Trans. Instrum. Meas. (2025).

[9] M. Wagdy Othman, Abdelhamied A. Ateya, Mohamed E. Nasr, Ammar Muthanna, Mohammed ElAffendi, Andrey Koucheryavy, Azhar A. Hamdi, Key enabling technologies for 6g: The role of uavs, terahertz communication, and intelligent reconfigurable surfaces in shaping the future of wireless networks, J. Sens. Actuator Netw. 14 (2) (2025) 30.

[10] Imen Jarraya, Abdulrahman Al-Batati, Muhammad Bilal Kadri, Mohamed Abdelkader, Adel Ammar, Wadii Boulila, Anis Koubaa, Gnss-denied unmanned aerial vehicle navigation: analyzing computational complexity, sensor fusion, and localization methodologies, Satell. Navig. 6 (1) (2025) 9.

[11] Christian Brommer, Alessandro Fornasier, Martin Scheiber, Jeff Delaune, Roland Brockers, Jan Steinbrener, Stephan Weiss, The insane dataset: Large number of sensors for challenging uav flights in mars analog, outdoor, and out-/indoor transition scenarios, Int. J. Robot. Res. 43 (8) (2024) 1083–1113.

[12] N.H. Riyaz Khan, S. Vasantha Kumar, Terrestrial lidar derived 3d point cloud model, digital elevation model (dem) and hillshade map for identification and evaluation of pavement distresses, Results Eng. 23 (2024) 102680.

[13] Siti Nur, Precision without gps: Multi-sensor fusion for autonomous drone navigation in complex environments, Int. J. Innov. Res. Comput. Sci. Technol. 12 (6) (2024).

[14] Muddesar Iqbal, Azam Rafique Memon, Dhafer J. Almakhles, Accelerating resource-constrained swarm robotics with cone-based loop closure and 6g communication, IEEE Trans. Intell. Transp. Syst. (2025).

[15] Naigui Xiao, Weisong Wen, Jiahao Hu, Peiwen Yang, Jiaqi Zhao, Chunjun Wu, Shiyu Bai, Sug-uav multirotor dataset with multi-sensor integration in indoor and urban areas, in: 2024 14th International Conference on Indoor Positioning and Indoor Navigation (IPIN), IEEE, 2024, pp. 1–5.

[16] Lovro Marković, Marin Kovač, Robert Milijas, Marko Car, Stjepan Bogdan, Error state extended Kalman filter multi-sensor fusion for unmanned aerial vehicle localization in gps and magnetometer denied indoor environments, in: 2022 International Conference on Unmanned Aircraft Systems (ICUAS), IEEE, 2022, pp. 184–190.

[17] Wenjia Xu, Yaxuan Yao, Jiaqi Cao, Zhiwei Wei, Chunbo Liu, Jiuniu Wang, Mugen Peng, Uav-visloc: A large-scale dataset for uav visual localization, arXiv preprint, arXiv:2405.11936, 2024.

[18] Deepak Prasad, S. Thanikai Adhithiyan, Kondru Thanmai, Gourinath Banda, Paveds: A synthetic dataset for developing autonomous personal aerial vehicles, IEEE Access (2023).

[19] Hui Ye, Rajshekhar Sunderraman, Shihao Ji, Uav3d: A large-scale 3d perception benchmark for unmanned aerial vehicles, arXiv preprint, arXiv:2410.11125, 2024.

[20] Gennaro Pio Rimoli, Francesco Palmieri, Massimo Ficco, Synthetic threat dataset generation by uav fleet simulation, 2024.

[21] Mehrnaz Sabet, Praveen Palanisamy, Sakshi Mishra, Scalable modular synthetic data generation for advancing aerial autonomy, Robot. Auton. Syst. 166 (2023) 104464.

[22] Hyeon Joong Wi, In Sung Jang, Ahyun Lee, Driving altitude generation method with pseudo-3d building model for unmanned aerial vehicles, ETRI J. 45 (2) (2023) 240–253.

[23] hailong1610 (Kaggle), UAV-VisLoc: A large-scale dataset for uav visual localization, https://www.kaggle.com/datasets/hailong1610/uav-visloc-dataset, 2024.

[24] Václav Pritzl, Matouš Vrba, Petr Štěpán, Martin Saska, Fusion of visual-inertial odometry with lidar relative localization for cooperative guidance of a micro-scale aerial vehicle, arXiv preprint, arXiv:2306.17544, 2023.

[25] OpenDroneMap Contributors, Opendronemap: Open source drone mapping software, https://www.opendronemap.org, 2022.

[26] T. Tomoji, Rtklib: An open source program package for gnss positioning, 2018.

[27] U.S. Geological Survey, USGS earthexplorer, https://earthexplorer.usgs.gov/, 2023.

[28] Clive Coetzee, The View from Space: Economic Applications of Remote Sensing: A Beginner's Guide, African Sun Media, 2024.

[29] Ashok K. Singh, Remote sensing of sustainability, in: Quantitative Assessment of Sustainability and Sustainable Development: Principles, Processes, and Challenges, Springer, 2025, pp. 173–212.

[30] Joseph Kevin McDuff, Armin Agha Karimi, Zahra Gharineiat, Enhancing spatial awareness and collaboration: A guide to vr-ready survey data transformation, ISPRS Int. J. Geo-Inf. 14 (2) (2025).

[31] Nicolo Dell'Unto, Giacomo Landeschi, Archaeological 3D GIS, Routledge, Taylor & Francis Group, 2022.

[32] Constantinos Heracleous, Panayiotis Kolios, D4.1b – overview of currently used and possible technical solutions for data analysis and data sharing, including common practices: Assessment and recommendations for future use, 2024.

[33] DroneDeploy Inc, Dronedeploy mapping and inspection platform, https://www.dronedeploy.com, 2023.

[34] Dhruvesh Patel, Raviraj Dave, Amit Kumar Dubey, Praveen Kumar Gupta, Raghavendra Singh, High-resolution dem creation using a uav for flood inundation hydrodynamic modeling-a case of rel river flood, Gujarat, India, in: EGU General Assembly Conference Abstracts, 2020, p. 5448.

[35] Yiqing Wan, A comparison between low-cost and professional rtk equipment under forest conditions, 2024.

[36] S.Z.A. Ismah, M.N. Cahyadi, A.B. Raharjo, F. Taufany, R. Mardiyanto, Integration of android application and gnss module for geographic information system (gis) of assets in near real-time, Earth Sci. Inform. 18 (4) (2025) 331.

[37] İsmail Melih Canbolat, High-density and homogeneous mapping using a motion controlled lidar, Master's thesis, Middle East Technical University, Turkey, 2023.

[38] Valeria-Ersilia Oniga, Ana-Maria Loghin, Mihaela Macovei, Anca-Alina Lazar, Bogdan Boroianu, Paul Sestras, Enhancing lidar-uas derived digital terrain models with hierarchic robust and volume-based filtering approaches for precision topographic mapping, Remote Sens. 16 (1) (2023) 78.

[39] Jesús García, Jose M. Molina, Simulation in real conditions of navigation and obstacle avoidance with px4/gazebo platform, Pers. Ubiquitous Comput. 26 (4) (2022) 1171–1191.

[40] Jessica Giovagnola, Juan B. Moro Megías, Miguel Molina Fernández, Manuel Pegalájar Cuéllar, Diego P. Morales Santos, Airloop: A simulation framework for testing of uav services, IEEE Access 11 (2023) 23309–23325.

[41] Kaiwen Wang, Lammmert Kooistra, Ruoxi Pan, Wensheng Wang, João Valente, Uav-based simultaneous localization and mapping in outdoor environments: A systematic scoping review, J. Field Robot. 41 (5) (2024) 1617–1642.

[42] Jiuhong Xiao, Daniel Tortei, Eloy Roura, Giuseppe Loianno, Long-range uav thermal geo-localization with satellite imagery, in: 2023 IEEE/RSJ International Conference on Intelligent Robots and Systems (IROS), IEEE, 2023, pp. 5820–5827.

[43] Christian Brommer, Alessandro Fornasier, Martin Scheiber, Jeff Delaune, Roland Brockers, Jan Steinbrener, Stephan Weiss, Insane: Cross-domain uav data sets with increased number of sensors for developing advanced and novel estimators, arXiv preprint, arXiv:2210.09114, 2022.

[44] Yuhang Wang, Xuefeng Feng, Feng Li, Qinglong Xian, Zhen-Hong Jia, Zongdong Du, Chang Liu, Lightweight visual localization algorithm for uavs, Sci. Rep. 15 (1) (2025) 6069.

[45] Xinyi Shi, Hao Wang, Zhengyou Zhang, Gang Yu, Gral: A uav dataset for geo-localization and beyond, in: Proceedings of the IEEE International Conference on Robotics and Automation (ICRA), 2019, pp. 2936–2942.

[46] Coraline Wyard, Benjamin Beaumont, Taïs Grippa, Eric Hallot, Uav-based landfill land cover mapping: optimizing data acquisition and open-source processing protocols, Drones 6 (5) (2022) 123.

[47] Rouwan Wu, Xiaoya Cheng, Juelin Zhu, Xuxiang Liu, Maojun Zhang, Shen Yan, Uavd4l: A large-scale dataset for uav 6-dof localization, arXiv preprint, arXiv:2401.05971, 2024.

[48] Yuwen Yao, Cheng Sun, Tao Wang, Jianxing Yang, Enhui Zheng, Uav geo-localization dataset and method based on cross-view matching, Sensors 24 (21) (2024) 6905.

[49] Bhavit Patel, Timothy D. Barfoot, Angela P. Schoellig, Visual localization with Google earth images for robust global pose estimation of uavs, in: 2020 IEEE International Conference on Robotics and Automation (ICRA), IEEE, 2020, pp. 6491–6497.

[50] Shuxiao Chen, Xiangyu Wu, Mark W. Mueller, Koushil Sreenath, Real-time geo-localization using satellite imagery and topography for unmanned aerial vehicles, in: 2021 IEEE/RSJ International Conference on Intelligent Robots and Systems (IROS), IEEE, 2021, pp. 2275–2281.

[51] Marius-Mihail Gurgu, Jorge Peña Queralta, Tomi Westerlund, Vision-based gnss-free localization for uavs in the wild, in: 2022 7th International Conference on Mechanical Engineering and Robotics Research (ICMERR), IEEE, 2022, pp. 7–12.

[52] Qi Yan, Jianhao Zheng, Simon Reding, Shanci Li, Iordan Doytchinov, Crossloc: Scalable aerial localization assisted by multimodal synthetic data, in: Proceedings of the IEEE/CVF Conference on Computer Vision and Pattern Recognition, 2022, pp. 17358–17368.

[53] Ivan Cisneros, Peng Yin, Ji Zhang, Howie Choset, Sebastian Scherer, Alto: A large-scale dataset for uav visual place recognition and localization, arXiv preprint, arXiv:2207.12317, 2022.

[54] Menghua Zhai, Zihang Bessinger, Scott Workman, Nathan Jacobs, Predicting ground-level scene layout from aerial imagery, in: Proceedings of the IEEE Conference on Computer Vision and Pattern Recognition (CVPR), 2017, pp. 867–875.

[55] Zhedong Zheng, Yunchao Wei, Yi Yang, University-1652: A multi-view multi-source benchmark for drone-based geo-localization, in: Proceedings of the 28th ACM International Conference on Multimedia, 2020, pp. 1395–1403.

[56] Janez Lapajne, Andrej Vončina, Ana Vojnović, Daša Donša, Peter Dolničar, Uroš Žibrat, Field-scale uav-based multispectral phenomics: Leveraging machine learning, explainable AI, and hybrid feature engineering for enhancements in potato phenotyping, Comput. Electron. Agric. 229 (2025) 109746.

[57] Natascha Oppelt, Arnab Muhuri, 5 fundamentals of remote sensing for terrestrial, in: Remote Sensing Handbook, Volume I: Sensors, Data Normalization, Harmonization, Cloud Computing, and Accuracies, 2024, p. 173.

[58] D.D. Khainus, R.M. Stupen, E. Makrickiene, I.I. Sadovyy, A.O. Siedov, Geospatial database generation of forest growth using the qgis software package, IOP Conf. Ser. Earth Environ. Sci. 1415 (2024) 012049.

[59] Sameer Mandal, V. Nunchhani, Arnab Bandyopadhyay, Aditi Bhadra, Development of qgis plugin for flood inundation mapping: applying otsu's thresholding technique, Sustain. Water Res. Manag. 11 (1) (2025) 1–13.

[60] M. Abdelkader, A.S. Al-Batati, A. Koubaa, ROS 2 key challenges and advances: A survey of ROS 2 research, libraries, and applications, 2024, 2024101204.

[61] Gang Peng, Tin Lun Lam, Chunxu Hu, Yu Yao, Jintao Liu, Fan Yang, Introduction to ROS 2 and programming foundation, in: Introduction to Intelligent Robot System Design: Application Development with ROS, Springer, 2023, pp. 541–566.

[62] Mattia Gramuglia, Giri Mugundan Kumar, Giorgio A. Orlando, Andrea L'Afflitto, An open-source framework to design, tune, and fly nonlinear control systems for autonomous uavs, in: AIAA SCITECH 2025 Forum, 2025, p. 2798.

[63] Tianxing Chen, Jiasheng Zhao, Zhiwei Hou, Hongbo Chen, Xuebin Zhuang, Distributed formation tracking for multi-uavs with unknown disturbances under event-triggered communication, J. Franklin Inst. (2024) 106997.

[64] Mohamed Abdelkader, Khaled Gabr, uav_dataset_generation_ros, https://github.com/mzahana/uav_dataset_generation_ros, January 2024. (Accessed January 2024).